TITLE

Evidence for increased fitness of a plant pathogen conferred by epigenetic variation

Authors

Rekha Gopalan-Nair[1], Aurore Coissac[1], Ludovic Legrand[1], Céline Lopez-Roques[2], Yann Pécrix[4], Céline Vandecasteele[2], Olivier Bouchez[2], Xavier Barlet[1], Anne Lanois[3], Alain Givaudan[3], Julien Brillard[3], Stéphane Genin[1] and Alice Guidot*[,1]

Addresses

[1]LIPME, Université de Toulouse, INRAE, CNRS, Castanet-Tolosan, France

[2]GeT-PlaGe, Genotoul, INRAE, US 1426, Castanet-Tolosan, France

[3]DGIMI, Université de Montpellier, INRAE, CNRS, Montpellier, France

[4]PVBMT, Université de La Réunion, CIRAD, Saint-Pierre, France

***Corresponding author:**

E-mail: alice.guidot@inrae.fr

ORCID: 0000-0001-5282-4157

Abstract

Adaptation is usually explained by adaptive genetic mutations that are transmitted from parents to offspring and become fixed in the adapted population. However, more and more studies show that genetic mutation analysis alone is not sufficient to fully explain the processes of adaptive evolution and report the existence of non-genetic (or epigenetic) inheritance and its significant role in the generation of adapted phenotypes. In the present work, we tested the hypothesis of the role of DNA methylation, a form of epigenetic modification, in adaptation of the plant pathogen *Ralstonia solanacearum* to the host plant during an experimental evolution. Using SMRT-seq technology, we analyzed the methylomes of 31 experimentally evolved clones that were obtained after serial passages on a given host plant during 300 generations, either on susceptible or tolerant hosts. Comparison with the methylome of the ancestral clone revealed between 12 and 21 differential methylated sites (DMSs) at the GTWWAC motif in the evolved clones. Gene expression analysis of the 39 genes targeted by these DMSs revealed limited correlation between differential methylation and differential gene expression. Only one gene showed a correlation, the RSp0338 gene encoding the EpsR regulator protein. The MSRE-qPCR (Methylation Sensitive Restriction Enzyme - qPCR) technology was used as an alternative approach to assess the methylation state of the DMSs found by SMRT-seq between the ancestral and evolved clones. This approach also found the two DMSs upstream of RSp0338. Using site-directed mutagenesis, we demonstrated the contribution of these two DMSs in host adaptation. As these DMSs appeared very quickly in the experimental evolution, we hypothesize that such fast epigenetic changes can allow rapid adaptation to the plant stem environment. To our knowledge, this is the first study showing a link between epigenetic variation and evolutionary adaptation to new environment.

Introduction

Faced with the selection pressure imposed by their environment, pathogens must continuously adapt to survive and multiply. Many works aim to better understand the adaptive processes of pathogens in order to better apprehend the sustainability of the control strategies. Adaptation, the modification of the phenotype as a result of natural selection, is usually explained by adaptive genetic mutations that are transmitted from parents to offspring and become fixed in the adapted population (Lenski 2017; Xue et al. 2019; Gatt and Margalit 2021). However, more and more studies show that genetic mutation analysis alone is not sufficient to fully explain the processes of adaptive evolution and report the existence of non-genetic (or epigenetic) inheritance and its significant role in the generation of adapted phenotypes (Lind and Spagopoulou 2018; Danchin et al. 2019). Epigenetic changes were described to be more involved in short-term adaptation, or acclimation, by inducing phenotypic plasticity (Vogt 2023). This was supported by the observation that epigenetic changes occur at a faster rate than genetic mutations but may be less stable (van der Graaf et al. 2015; Walworth et al. 2021). However, recent works also support the hypothesis that epigenetic modifications could impact long-term adaptive responses to changing environments through the transgenerational inheritance of epigenetic signatures (Kronholm and Collins 2016; Kronholm et al. 2017; Danchin et al. 2019; Stajic et al. 2019; Walworth et al. 2021; Vogt 2023).

A well-documented epigenetic mechanism known to be involved in the modification of the phenotypes is DNA methylation. DNA methylation consists in the addition of a methyl group (CH_3) on the adenine or cytosine base of DNA catalyzed by DNA methyltransferases (MTases) that will recognize a specific DNA motif. In bacterial genomes, methylated DNA is found in the forms of 6mA (6-methyladenine), which is the most prevalent form; 4mC (4-methylcytosine) and 5mC (5-methylcytosine) (Clark et al. 2012; Blow et al. 2016). Many works demonstrated the role of DNA methylation in the regulation of important cellular functions in bacteria, including DNA replication, DNA repair, chromosome segregation, transcriptional regulation, phenotypic heterogeneity and virulence (Casadesús and Low

2006; López-Garrido and Casadesús 2010; Estibariz et al. 2019; Nye et al. 2019; Payelleville et al. 2019; Sánchez-Romero and Casadesús 2020; Oliveira and Fang 2021). Nowadays, thanks to the Pacbio sequencing technology enabling sequencing of single molecules in real time (SMRT-seq) without amplification, it is now possible to analyze the global DNA methylation profile (methylome) of bacteria (Clark et al. 2012; Murray et al. 2012; Davis et al. 2013; Blow et al. 2016; Beaulaurier et al. 2019). Here, we used SMRT-seq technology to explore the methylome of the model bacterial plant pathogen *Ralstonia solanacearum.* The purpose of this study was to test the hypothesis of methylome variation during an experimental adaptation of the bacteria to various host plants and the potential role of methylome changes in the generation of adapted phenotypes.

R. solanacearum is a soil-born plant pathogen responsible of the lethal bacterial wilt disease on more than 250 plant species including economically important crops such as tomato, potato or banana (Vailleau and Genin 2023). This bacterium is worldwide distributed and represents a major threat in agriculture. It is characterized by a strong adaptive capacity, no effective control method is available today and new strains able to colonize new hosts are continuously emerging (Wicker et al. 2007; Wicker et al. 2009; Lopes et al. 2015; Jiang et al. 2016; Bergsma-Vlami et al. 2018). Many works investigated in a better understanding of the adaptive processes in *R. solanacearum*. The role of genetic modifications of the bacterial genome such as mutation, transposable elements movement, recombination or horizontal gene transfer were reported (Coupat-Goutaland et al. 2011; Wicker et al. 2012; Lefeuvre et al. 2013; Guidot et al. 2014). However, the contribution of epigenetic modifications in *R. solanacearum* adaptation has not yet been addressed.

A recent study compared the methylomes using SMRT-seq of two *R. solanacearum* strains belonging to distant phylogenetics groups, the GMI1000 strain from phylotype I and the UY031 strain from phylotype II (Erill et al. 2017). This work identified a commonly methylated motif in the two strains, the GTWWAC motif, 6mA methylated, associated with a MTase, M.RsoORF1982P, that is conserved in all

92 complete *Ralstonia* spp. genomes and across the *Burkholderiaceae* (Erill et al. 2017). Analysis of the
93 methylated regions in *R. solanacearum* genomes identified genes involved in global and virulence
94 regulatory functions thus suggesting a role of DNA methylation in regulation of their expression.

95 In our previous works, we conducted an experimental evolution of the *R. solanacearum* GMI1000
96 strain in order to better understand the molecular bases of adaptation. In this experiment, strain GMI1000
97 was maintained in a fixed plant line during 300 generations by serial passages from stem to stem. This
98 experiment was conducted on six different plant species including susceptible hosts (tomato var.
99 Marmande, eggplant var. Zebrina, pelargonium var. Maverick Ecarlate) and tolerant hosts (bean var. Blanc
100 Précoce, cabbage var. Bartolo, tomato var. Hawaii 7996) (Guidot et al. 2014; Gopalan-Nair et al. 2020).
101 Most of the evolved clones showed a better fitness in their experimental host than the ancestral clone.
102 Whole genome sequence analysis revealed between zero and three mutations in the adapted clones and
103 the role of some mutations in host adaptation was demonstrated (Guidot et al. 2014; Perrier et al. 2016;
104 Perrier et al. 2019; Gopalan-Nair et al. 2020). However, in several adapted clones no mutation could be
105 detected, suggesting that epigenetic modifications may play a role in host adaptation. In addition,
106 transcriptomic analysis of these clones revealed important differential gene expression compared to the
107 ancestral clone, thus reinforcing the hypothesis of a role of epigenetic modification in gene expression
108 change (Gopalan-Nair et al. 2020; Gopalan-Nair et al. 2023).

109 In this study, we analyzed the methylomes of 31 experimentally evolved clones using SMRT-seq.
110 Comparison with the methylome of the ancestral GMI1000 clone revealed differential methylated sites
111 (DMSs) at the GTWWAC motif in the evolved clones. Using site-directed mutagenesis, we demonstrated
112 the contribution of one DMS in host adaptation, which, interestingly, turns out to be linked to a gene
113 involved in the expression of a bacterial virulence determinant.

114

Materials and methods

Bacterial strains, plant material and growth conditions

The GMI1000 strain and the 31 derived evolved clones investigated in this study are described in table 1. The evolved clones generated after experimental evolution include ten clones evolved in tomato Hawaii 7996 (*Solanum lycopersicum*) (Gopalan-Nair et al. 2020), seven clones in eggplant MM61 (*S. melongena* var. Zebrina), three clones in bean (*Phaseolus vulgaris* var. Blanc Précoce), six clones in tomato Marmande (*S. lycopersicum* var. Super Marmande), and five clones in cabbage (*Brassica oleracea* var. Bartolo) (Guidot et al. 2014). The bacterial strains were grown at 28°C (under agitation at 180 rpm for liquid cultures) either in BG complete medium or in MP synthetic medium (Plener et al. 2010). The pH of the MP medium was adjusted to 6.5 with KOH. For agar plates, BG medium was supplemented with D-Glucose (5 g/l) and triphenyltetrazolium chloride (0.05 g/l). The MP medium was supplemented with L-Glutamine (10 mM) and oligo elements (1000 mg/l) (Gopalan-Nair et al. 2023).

Four to five-week-old tomato (*Solanum lycopersicum*) cultivar Marmande plants were used for the *in planta* bacterial competition assays. Tomato plants were grown in a greenhouse. *In planta* competition experiments were conducted in a growth chamber under the following conditions: 12 h light at 28°C, 12 h darkness at 27°C and 75% humidity.

SMRT-seq

Genomic DNA was prepared from the bacterial cells grown in synthetic media with glutamine collected at the beginning of stationary phase in order to limit the number of cells in division and avoid a bias towards hemimethylated marks. The bacterial samples were collected as described previously (Gopalan-Nair et al. 2020). Briefly, each of the evolved clones and the ancestral clone GMI1000 were grown in MP medium with 10mM glutamine. For whole genome sequencing, 20 ml of the bacterial culture was centrifuged at 5000g for 10 minutes followed by washing the pellets with water and centrifuged again. The pellets were

stored at -80°C until DNA extraction. The DNA were prepared based on the protocol described for high molecular weight genomic DNA (Mayjonade et al. 2017).

Library preparation was performed at GeT-PlaGe core facility, INRAE Toulouse, France and SMRT sequencing at Gentyane core facility, INRAE Clermont-Ferrand, France. Eight libraries of multiplex samples were performed according to the manufacturer's instructions "Procedure-Checklist-Preparing-Multiplexed-Microbial-SMRTbell-Libraries-for-the-PacBio-Sequel-System." At each step, DNA was quantified using the Qubit dsDNA HS Assay Kit (Life Technologies) and DNA purity was tested using the nanodrop (Thermo Fisher Scientific). Size distribution and degradation were assessed using the Fragment analyzer (AATI) and High Sensitivity Large Fragment 50 kb Analysis Kit (Agilent). Purification steps were performed using AMPure PB beads (PacBio). The 32 individual samples (2 µg) were purified, then sheared at 10 kb using the Megaruptor1 system (Diagenode). Using SMRTBell template Prep Kit 1.0 and SMRTbell Barcoded Adaptater kit 8A or 8B kits (PacBio), samples (1 µg) were independently barcoded then pooled by 5 to 8. The 8 libraries were purified tree times. SMRTbell libraries were sequenced on SMRTcells on Sequel1 instrument at 6pM with 120-min preextension and 10-h or 20h movies using Sequencing Primer V4, polymerase V3, diffusion loading.

GTWWAC methylation analysis

All methylation analyses were performed with public GMI1000 genome and annotation. Motif and methylation detection were performed using the pipeline "pbsmrtpipe.pipelines.ds_modification_motif_analysis" from PacBio SMRTLink 6.0. The default settings were used except: compute methyl fraction set as true, minimum required alignment concordance >= 80 and minimum required alignment length >= 1000.

Followed by the bioinformatics analyses of the data obtained from SMRT sequencing, methylome profiles of the 31 evolved clones were compared to the ancestral clone individually. The analysis showed

the methylation profile for G**T**WWAC motif with a score, coverage, IPD ratio, and fraction for each sample. A score above 30 is considered significant and coverage represents the sequencing depth (higher the better). IPD ratio or interpulse duration ratio is the time required for the consequent nucleotide to bind, where the presence of methylated base increases the time required for the nucleotide addition (higher IPD ratio means a higher probability of methylation). The fraction represents the percentage of methylated bases in the genome pool at that particular position. In this experiment, the methylation or hemimethylation of a particular position is considered significant when the fraction is greater than or equal to 0.50 (represents at least 50% of the sequences are methylated at that particular position in the whole genome pool) in addition to the score above 30.

MSRE-qPCR

The MSRE-qPCR (Methylation Sensitive Restriction Enzyme – quantitative PCR) approach was used to check the methylation profile at a specific genomic region (Krygier et al. 2016). The protocol used for MSRE-qPCR derived from Payelleville et al. (2019). Genomic DNA was extracted from bacterial cells grown in the same culture condition (synthetic MP medium with glutamine) and at the same growth stage (beginning of stationary phase) used for SMRT-seq. Genomic DNA extraction and purification was performed using the Genomic DNA Purification Kit from Promega. First, in order to generate numerous linear DNA fragments, 400 ng of genomic DNA was digested by *Eco*RI (0.25U in a total volume of 20µL) for one night at 37°C followed by an enzyme inactivation step (20 min at 65˚C). Then, 8 µl of *Eco*RI-digested-DNA was digested by *Hpy166*II (0.25U in a total volume of 20 µL) for one night at 37°C followed by an enzyme inactivation step (20 min at 65˚C). The *Hpy166*II restriction enzyme digests only unmethylated GTNNAC sites. A qPCR amplification was then performed on 2 µl of 10^{-5} diluted DNA in a total volume of 7 µl containing 3.6 µl of Master mix Takyon SYBR Green I and 0.5 mM of each primer. Primers used for MSRE-qPCR are described in supplementary Table S1. The qPCR amplification was performed using the

187 LightCycler 480 II (Roche) and the following program ; 3 min of denaturation at 95°C, and 45 cycles of
188 denaturation 10 sec at 95°C and primer annealing 45 sec at 65°C. Detection of an amplicon revealed that
189 no digestion occurred and that the region was methylated, while non amplification revealed that the
190 region was unmethylated and digested. The mAG4 mutant (GMI1000 deleted from the RSc1982 MTase,
191 targeting GTWWAC motifs; see mutant construction below) was used as a non-methylated control at
192 GTWWAC motifs (a negative control for qPCR amplification). *Eco*RI digested DNA diluted 10^{-5} times was
193 used as a positive control for qPCR amplification.

194 Raw data from qPCR experiments were analyzed using the $2^{-\Delta\Delta Ct}$ method to perform a relative
195 quantification (Livak and Schmittgen 2001). This method was used to relate the PCR signal of the MSRE
196 digested DNA to the PCR signal of the *Eco*RI digested DNA. Ct values obtained with MSRE-digested DNA
197 were first normalized with Ct values obtained with *Eco*RI-digested DNA ($\Delta Ct = Ct_{MSRE\text{-}DNA} - Ct_{EcoRI\text{-}DNA}$). This
198 ΔCt value was then normalized with the ΔCt value obtained with GMI1000 DNA ($\Delta\Delta Ct = \Delta Ct_{evolved.clone} -$
199 $\Delta Ct_{GMI1000}$). This ΔΔCt value was then normalized by the amplification efficiency coefficient of the target
200 and reference DNAs. Here, we estimated that the two DNAs had the same amplification efficiency and
201 close to one. Therefore, the amount of target, normalized to the reference and relative to the calibrator,
202 was given by the $2^{-\Delta\Delta Ct}$ value (Livak and Schmittgen 2001). Three biological replicates (DNA extracted from
203 independent bacterial cultures) and three technical replicates (three qPCR experiments per DNA sample)
204 were performed. The $2^{-\Delta\Delta Ct}$ values were compared using the Wilcoxon non-parametric test with the R
205 software.

206

207 ## Construction of mutants

208 The mAG4 mutant (GMI1000 deleted from the RSc1982 MTase gene) was constructed using a SacB
209 protocol as described in Gopalan-Nair et al. (2020). At the end of the protocol, gene deletion was checked

by PCR on colonies that were resistant to sucrose and sensitive to kanamycine (plasmid lost with second recombination event).

Point mutations of the two GTWWAC motifs, changing the T by a C, upstream the RSp0338 gene were performed using the gene replacement method with the pK18 plasmid containing the *sacB* counter-selectable marker, as previously described (Gopalan-Nair et al. 2020). All the point mutations were performed on both the ancestral clone and the Mar26b2 evolved clone. All mutants were tagged with the fluorescent reporters mCherry or GFP as previously described (Perrier et al. 2019). The primers used for the construction of mutants are listed in Table S1.

RT-qPCR analysis

The RT-qPCR (Reverse Transcription – quantitative PCR) approach was used to quantify the expression of the *epsR* gene in the ancestral GMI1000 clone, the evolved clones and the GTWWAC-epsR mutants. The protocol used for RT-qPCR derived from Perrier et al. (2016). Total RNA were isolated using TRIzol Reagent (life technologies) followed by RNeasy MiniElute Cleanup Kit (Qiagen). To avoid contamination by genomic DNA each sample was treated with the TURBO DNA-free Kit (life technologies). The reverse transcription was performed on 1 µg of total RNA using the Transcriptor Reverse Transcriptase (Roche) with random hexanucleotides primers. Quantitative PCRs were performed on a Roche LightCycler480 using The LightCycler® 480 SYBR Green I Master (Roche). Cycling conditions were as follows: 95°C for 5 min, 45 cycles at 95°C for 15 s, 60°C for 20 s and 72°C for 20 s. The specificity of each amplicon was validated with a fusion cycle. The efficiency of amplification was tested with dilution game and calculated using $-1+10^{1/slope}$ formula. The expression of *epsR* was normalized using the geometric average of three selected reference genes (RSc0403, RSc0368 and RSp0272) for each sample and calculated using the $2^{-\Delta\Delta Ct}$ method (Livak and Schmittgen 2001; Rao et al. 2013). All kit and reagents were used following the manufacturer's recommendations. The primer sets used in the experiments are listed in Table S1.

Bacterial competition assay and serial passage experiment

The bacterial competitive assay was performed as previously described (Perrier et al. 2019). Briefly, 10 µl of the mixed inoculum, containing the GFP and mCherry clones in equal proportion at a 10^6 CFU/ml concentration, was injected into the stem of tomato cv. Marmande, 1 cm above the cotyledons. Bacteria were recovered from the plant stem as soon as the first wilting symptoms appeared (3-5 days after inoculation) as previously described (Guidot et al. 2014).

Four serial passage experiments (SPE) into the stem of tomato cv. Marmande were performed. At each SPE, serial dilutions of the recovered bacterial suspension were conducted. Ten microliter of the 10^{-3} dilution was directly injected into the stem of a healthy plant and 50 µl of the 10^{-4} and 10^{-6} dilutions were plated on BG complete medium without triphenyltetrazolium chloride using an automatic spiral plater (easySpiral, Interscience, France). Green and red colonies were visualized and enumerated using a fluorescence stereo zoom microscope (Axio Zoom.V16, ZEISS, Germany). A competitive index (CI) was calculated at each SPE as the ratio of the two clones obtained from the plant stem (output) divided by the ratio in the inoculum (input) (Macho et al. 2010). A total of seven replicates were performed for each competition assay. Differences between mean CI values were tested using a Wilcoxon test performed in the R statistical software.

Results

Defining the 6mA methylation profile of strain GMI1000

In order to detect potential changes in the methylation profile of evolved clones, we first established the 6mA modification sites in the wild-type ancestor GMI1000. Methylation of 6mA type at the GTWWAC motif was investigated using SMRT-seq technology. In order to limit the number of cells in division and

avoid a bias towards hemimethylated marks, genomic DNA was prepared from bacterial cells collected at the beginning of stationary phase. Growth was performed in synthetic medium with glutamine to mimic xylemic environment of the plant, glutamine being the main compound of xylem sap in most plant species (Baroukh et al. 2022).

A total of 392 GTWWAC motifs are present on the GMI1000 genome. In our culture and growth phase conditions and according to SMRT-seq data, 10 GTWWAC motifs were detected unmethylated in the GMI1000 genome, four on the chromosome and six on the megaplasmid (Table 2 and Supplemental Table S2). Eight of these unmethylated motifs were located in the upstream region of a gene, thus potentially affecting gene expression. This specifically concerned the RSc0958 gene encoding a type VI secretion system tip VgrG family protein, the *epsR* gene (two motifs) encoding the negative regulator of exopolysaccharide production (Chapman and Kao 1998) and the *efe* gene encoding the Ethylene-forming enzyme (Valls et al. 2006). We also identified 9 motifs that were hemimethylated (DNA methylation of either strand – or strand +) in the GMI1000 genome (Table 2 and Supplemental Table S2).

Mapping differential methylated sites between the ancestral and evolved clones with SMRT-sequencing

A total of 31 evolved clones derived from strain GMI1000 after experimental evolution in 5 different host plants over 300 generations were investigated. All clones but one exhibited a better fitness than their ancestral clone in their experimental host according to competition experiments (CI>1). Only the clone Zeb26d1 recovered from eggplant Zebrina had a CI not significantly different from one and was used as a control. An average of 1.2 (min 0 ; max 3) genomic polymorphisms were detected in these 31 evolved clones (Gopalan-Nair et al. 2023) (Table 1).

SMRT-seq data from the 31 evolved clones were investigated for methylome analysis, in similar conditions as for the ancestral clone. Comparison of the methylation marks on the adenine of the

GTWWAC motifs between the ancestral clone and the 31 evolved clones revealed a list of 50 DMSs. This list included 30 DMSs at one DNA strand (hemimethylated region) and 10 DMSs at both DNA strands (Tables 3a and 3b).

Characteristics of the DMSs

Methylome comparison between the ancestral clone and the 31 evolved clones revealed between 12 and 21 (15.5 ± 2.2 ; mean ± standard deviation) DMSs per evolved clone (Tables 3a,3b and Supplemental Figure 1). The experimental host did not have a strong impact on the number of DMSs, with the exception that the number of DMSs detected in bean clones was significantly superior to the number of DMSs detected in eggplant Zebrina and in tomato Hawaii clones (Supplemental Figure 1).

Genomic repartition analysis of the DMSs revealed that 26 were on the chromosome (3.7 Mb) and 24 on the megaplasmid (2.1 Mb) which seems to indicate a higher frequency on the second replicon (Table 4 and Figure 1). However, the examination of the map does not reveal any specific region enriched in hypo or hypermethylation (Figure 1).

DMSs can be classified as intragenic (position within a coding sequence), or intergenic either at the 5' (upstream) or 3' (downstream) position of a gene. Due to the existence of divergent promoters, a DMS at the 5' position can potentially affect two genes, which explains why the number of genes potentially affected by these DMSs (39 genes) is slightly different from the number of DMSs (Table 4). Clearly, the number of DMSs positioned in a gene promoter region (defined as less than 300 nucleotides from the start codon) of the 39 affected genes is predominant (78%). Interestingly, one regulatory gene (RSp0338) has two GTWWAC motifs in its promoter region, both differentially methylated on both DNA strands (Table 3b). An examination of the list of the DMSs affecting promoter regions revealed an overabundance of genes encoding transposable elements (33%) and genes closely or remotely associated

305 with virulence (*epsR*, *efe*, the type III effector *ripAA* and VGR-related proteins linked to the type VI
306 secretion system) (31%) (Table 4).
307
308 ## Differential methylation does not appear to be correlated with differential gene expression
309 Transcriptome analyses for the ancestral clone and the 31 evolved clones were performed by RNA
310 sequencing in our previous work (Gopalan-Nair et al. 2023). Table 5a gives a summary of the relative gene
311 expression in the experimentally evolved clones compared to the ancestral clone for each of the 39 genes
312 targeted by a DMS. A Fisher exact test was used to determine whether there was an association between
313 differential methylation and differential gene expression. This analysis revealed a significant correlation
314 only for the RSp0338 gene (Table 5b).
315 Down regulation of the RSp0338 gene in the Mar26b2, Bean26c1 and Cab36d1 clones compared
316 to the ancestral GMI1000 clone was investigated using a RT-qPCR approach. This analysis showed that the
317 RSp0338 gene is down-regulated in the three investigated evolved clones compared to the ancestral
318 GMI1000 clone (Figure 2).
319
320 ## Assessment of methylation status through the MSRE-qPCR approach
321 We used MSRE-qPCR (Methylation Sensitive Restriction Enzyme- quantitative PCR) assay as an alternative
322 approach to assess the methylation status of DMSs identified by SMRT-seq. Briefly, MSRE-qPCR is based
323 on extensive digestion of genomic DNA with methylation-sensitive restriction enzyme (MSRE) followed by
324 quantitative PCR amplification of the target gene (Krygier et al. 2016). With this method, we could only
325 test two-strand-DMSs, but not hemimethylated sites. Genomic DNA was prepared in similar conditions as
326 for SMRT-seq.
327 The MSRE-qPCR approach was first used to assess the methylation status of the GMI1000 strain
328 for three motifs that were detected methylated on both DNA strands for a majority of the evolved clones

329 but not methylated in the ancestral clone according to SMRT-seq. These three motifs were associated
330 with the RSc2612, RSc1329 and RSc1529 genes (Table 3). According to the MSRE-qPCR results, the
331 ancestral clone was found methylated such as the evolved clones (Figure 3).

332 We then used MSRE-qPCR to investigate the methylation status of seven motifs found
333 differentially methylated according to SMRT-seq. These seven motifs included one motif in the divergent
334 promoter region of both RSc0102 and RSc0103, two motifs upstream of RSp0338 and one motif upstream
335 of RSc0958, RSp0629, RSp1152 and RSp1643 (Tables 3a and 3b). MSRE-qPCR analysis was conducted on
336 both GMI1000 DNA and DNA from the evolved clones in which the two-strands-DMSs were found (Table
337 3a and 3b). For the RSp0338 and RSp0629 genes, we also included in the analysis DNA from three evolved
338 clones in which differential hemimethylation was detected. This concerned the Bean26c1 clone for
339 RSp0338 and Mar26a2 and Haw35a1 clones for RSp0629. According to the MSRE-qPCR results, the
340 GTWWAC motifs upstream of RSc0102/RSc0103, RSc0958, RSp0629, RSp1152 and RSp1643 were not
341 found differentially methylated between the ancestral and the evolved clones, being fully methylated in
342 both (Figure 4). However, the MSRE-qPCR analysis showed that the region upstream of RSp0338 was
343 differentially methylated between GMI1000 and the three independent clones evolved on tomato var.
344 Marmande, bean and cabbage. In agreement with SMRT-seq data, the GTWWAC motifs upstream of
345 RSp0338 appeared not methylated in the ancestral clone but methylated in the Mar26b2, Bean26c1 and
346 Cab36d1 evolved clones (Figure 4).
347

348 ## Methylation upstream of the RSp0338 gene appeared after only 2 passages in plant

349 In this part of the study, we were interested in determining at which evolution stage did the RSp0338
350 differential methylation arises. To answer this question, we conducted an MSRE-qPCR analysis on DNA
351 from clones from the tomato Marmande lineage B evolved after one, two, three, four, five, ten, 14, 18
352 and 22 serial passages. Two clones per serial passage were investigated. The MSRE-qPCR results showed

353 that the two GTWWAC motifs upstream RSp0338 were not methylated for the two clones recovered after
354 one passage, as for the ancestral clone. However, the motifs were already methylated in one of the two
355 clones recovered after two and three passages and remain methylated in all the clones recovered in the
356 following passages (Figure 5).
357
358 ## Methylation in the upstream region of RSp0338 contributes to bacterial fitness
359 In our previous work, we demonstrated that the Mar26b2 clone showed a fitness advantage during
360 growth into the stem of its experimental host, tomato var. Marmande, compared to the ancestral
361 GMI1000 clone, using a competition experiment approach (Table 1; Guidot et al. 2014).
362 In order to analyze the contribution of methylation in the upstream region of the RSp0338 gene
363 in fitness gain of the Mar26b2 clone into tomato var. Marmande, we first constructed mutants of both
364 GMI1000 and Mar26b2 strains in which the two GTWWAC motifs in the upstream region of RSp0338 were
365 modified, so that they can no longer be methylated. The GTWWAC motifs modification was performed by
366 introduction of a point mutation replacing the T by a C (Table 6). In a second step, we measured the impact
367 of these mutations on the bacterial fitness into tomato var. Marmande. Our hypothesis was that the
368 strains having a fitness advantage into tomato var. Marmande should enhance their frequency in the
369 population after serial passage experiments (SPE) in this host. We thus conducted SPE in tomato var.
370 Marmande starting with a mixed inoculum of the investigated clones and mutants and measured the
371 competitive index (CI) after each passage (Figure 6A). Competition SPE with the Mar26b2 and GMI1000
372 clones validated the fitness advantage of the Mar26b2 clone with CI values enhancing at each passage
373 (Figure 6B). Competition SPE with the GMI1000 mutant and GMI1000 wild-type strain showed that the CI
374 values were not significantly different from one at each passage, thus demonstrating that point mutations
375 of the GTWWAC motifs of the RSp0338 upstream region did not impact the fitness of the GMI1000 strain
376 (Figure 6C). Competition SPE with the Mar26b2 clone and Mar26b2 mutant showed an increase in CI

values at each passage (even if this increase was not as high as the increase observed for Mar26b2 and GMI1000 competition), thus demonstrating a fitness advantage of Mar26b2 clone compared to Mar26b2 mutant (Figure 6D). Considering that point mutations of the GTWWAC motifs of the RSp0338 upstream region did not impact the fitness (Figure 6C), these results showed a role of methylation of these GTWWAC motifs in adaptive advantage of Mar26b2 clone for growth into the stem of tomato var. Marmande.

Discussion

DNA methylation changes during experimental adaptation of *R. solanacearum* to multihost species

In our previous works, transcriptomic analyses of experimentally adapted clones of *R. solanacearum* to various host plants revealed important variations in gene expression even in clones with no genomic alteration (Gopalan-Nair et al. 2020; Gopalan-Nair et al., 2023). Here, we investigated the methylomes of these evolved clones using SMRT-seq technology, which identified a list of 50 putative differentially methylated sites at the GTWWAC motif with a varying number of 12 to 21 DMSs per evolved clone. This list included 30 differential hemimethylated (one DNA strand) and 10 differential methylated sites (both DNA strands). In bacteria, hemimethylated DNA is produced at every round of DNA replication. This DNA modification is generally transient because the DNA methyltransferases will quickly re-methylate the majority of their target motifs. However, stable hemimethylated and unmethylated motifs have been reported in various organisms including bacteria (Payelleville et al. 2018; Sharif and Koseki 2018; Sánchez-Romero and Casadesús 2020). This phenomenon is well documented in *E. coli* and *S. typhimurium* where stable hemimethylated and unmethylated GATC sites are formed when a DNA- binding protein protects hemimethylated DNA from Dam methylase activity (Sánchez-Romero and Casadesús 2020). Differential methylation pattern on the DNA are involved in phenotypic variation by impacting gene expression

400 through the differential affinity of some transcription factors for methylated *versus* unmethylated or
401 hemimethylated promoters (Casadesús and Low 2013).

402 The MSRE-qPCR approach was used as an alternative methodology to investigate the methylation
403 state of the 10 two-strand-DMSs detected by SMRT-seq. MSRE-qPCR appeared to be more stringent,
404 founding only a small proportion of the differential methylated sites detected by SMRT-seq. Only one
405 site, upstream of RSp0338, was detected between the ancestral clone and three evolved clones to be
406 differentially methylated by using the MSRE-qPCR approach. A technical reason may explain this
407 discrepancy, because restriction endonuclease sensitive to methylation can display various rates of
408 cleavage depending on several parameters (time of digestion, amount of enzyme, flanking sequence…),
409 and therefore do not always cut 100% of the DNA motifs they recognize (Roberts et al. 2015). Another
410 possible reason for this discrepancy could be dependent on phenotypic heterogeneity, which is common
411 in bacterial populations (Casadesús and Low 2013). This phenomenon has already been observed in
412 populations of *R. solanacearum* GMI1000 (Perrier et al. 2019) and several mechanisms involved in the
413 generation of phenotypic heterogeneity include epigenetic regulations (Casadesús and Low 2013; Parab
414 et al. 2022). This could explain why different methylation states were found using either the SMRT-seq or
415 MSRE-qPCR technologies. It should be remembered that MSRE-qPCR can only detect two-strand
416 methylated sites, unlike SMRT-seq, but it is likely that both methods generate false positives.
417 Nevertheless, SMRT-seq already provides a first comprehensive view of 6mA methylation profile of both
418 ancestral and evolved clones, and the combination of the two methods has enabled us to robustly validate
419 two differential methylation sites upstream RSp0338 between the ancestral and three evolved clones.
420

421 ## DNA methylation changes rarely correlate with changes in gene expression

422 Among the 31 investigated evolved clones, 39 genes had a potential DMS mark. The analysis of the
423 association between differential methylation and differential gene expression, however, revealed a

significant correlation only for the RSp0338 gene. This data supports a recent analysis of the *Salmonella typhimurium* methylome and transcriptome showing that DNA methylation changes generally do not correlate with obvious changes in gene expression (Bourgeois et al. 2022).

Concerning the RSp0338 gene, the two GTWWAC motifs that were detected as differentially methylated, are located 321 bp and 309 bp upstream the start codon, thus potentially affecting the promoter region. The correlation between differential methylation and differential expression of the RSp0338 gene suggested an epigenetic regulation, a phenomenon reported in prokaryotes although still scarcely investigated (Payelleville and Brillard 2021). Epigenetic regulation in bacteria was reported to result from the impact of DNA methylation on the interaction of DNA-binding proteins with their cognate sites or on changes in DNA topology (Casadesús and Low 2013; Casadesús 2016; Sánchez-Romero and Casadesús 2020). Here, we provide evidence that RSp0338 is a novel example of epigenetically regulated gene in bacteria.

Why adapt through methylation?

Epigenetic mutations are known to occur at a faster rate than genetic mutation (van der Graaf et al. 2015; Hu et al. 2019). The novel methylation state of the RSp0338 promoter appeared very quickly in the experimental evolution since they are detected from the first two or three serial passages on the hosts. We hypothesize that such fast epigenetic changes can allow rapid adaptation to new environmental conditions. There's also the plausibility that epimutation is easier to generate (and especially to revert) than a genetic mutation, and that this property is therefore favorable to rapid adaptation in fluctuating environments. A question that remains unanswered is the stability of the novel methylation profile and how it will influence long-term adaptation to new environments. More and more studies report the existence of stable ‘epialleles’ that are transmitted intergenerationally and affect the phenotype of offsprings. In the same way as conventional DNA sequence-based alleles, these epialleles could be

448 subjected to natural selection thus contributing to long-term evolutionary processes (Ashe et al. 2021).
449 Other studies support the hypothesis of the genetic assimilation theory by which epigenetic changes could
450 facilitate genetic mutation assimilation (Ehrenreich and Pfennig 2016; Kronholm and Collins 2016;
451 Kronholm et al. 2017; Danchin et al. 2019; Stajic et al. 2019; Walworth et al. 2021).
452

453 ## Evidence that methylation changes in RSp0338 (*epsR*) provides adaptation

454 Using a site-directed mutagenesis approach targeting the GTWWAC motifs that were detected
455 differentially methylated between the evolved clones and the ancestral clone, we prevented the
456 methylation by the MTase. An *in planta* competition experiment between the mutant and the evolved
457 clone demonstrated that methylation of the motifs in the upstream region of the RSp0338 gene gives an
458 adaptive advantage. To our knowledge, this is the first study showing a link between epigenetic variation
459 and evolutionary adaptation to new environment. The involvement of epigenetic variation in
460 environmental adaptation has been reported in several eukaryotic species (Weiner and Katz 2021; Vogt
461 2023). In bacteria, this has been reported for adaptation to antibiotic treatments (Ghosh et al. 2020;
462 Muhammad et al. 2022).

463 The Rsp0338 gene has been characterized in the past as *epsR* (Chapman and Kao 1998), but its
464 function remains unclear. EpsR, a putative DNA-binding protein, was shown to regulate exopolysaccharids
465 (EPS) production in *R. solanacearum* since its overproduction strongly represses EPS synthesis but
466 inactivation of the gene did not obviously affect EPS production (Chapman and Kao 1998; Garg et al. 2000).
467 Based on this knowledge, it is difficult to infer a role for the decrease in *epsR* expression (as suggested by
468 the transcriptomic data from evolved clones) linked to methylation of its promoter. Nevertheless, it is
469 certain that *epsR* is, directly or indirectly, linked to the PhcA-dependent virulence regulation network in
470 *R. solanacearum* (Garg et al. 2000; Genin and Denny 2012), and probably contributes to the control of EPS
471 production or associated molecules. It should be noted that during the evolution of GMI1000 by serial

472 passages on several host plants, alterations in another regulatory gene, *efpR*, conferring strong adaptive
473 gains were selected and lead to multiple phenotypic changes, including significant modifications for EPS
474 production (Perrier et al. 2016; Perrier et al. 2019). We can therefore hypothesize that the production of
475 these surface/excreted molecules plays an important role in the phases of adaptation to the
476 environmental conditions encountered during plant infection, and future work will need to establish their
477 role at this level.
478

479 ## Conflict of Interest

480 The authors declare that there are no conflicts of interest.
481

482 ## Funding information

483 This work was supported by the French National Research Agency (grant number ANR-17-CE20-0005-01)
484 and the "Laboratoires d'Excellence (LABEX)" TULIP (ANR-10-LABX-41). R.G.N was funded by a PhD
485 fellowship from the "Laboratoires d'Excellence (LABEX)" TULIP (ANR-10-LABX-41; ANR-11-IDEX-0002-02).
486 This work was performed in collaboration with the GeT core facility, Toulouse, France (DOI :
487 10.17180/nvxj-5333) (http://get.genotoul.fr) and was supported by France Génomique National
488 infrastructure, funded as part of "Investissement d'avenir" program managed by the French National
489 Research Agency (ANR-10-INBS-09) and by the GET-PACBIO program (« Programme operationnel FEDER-
490 FSE MIDI-PYRENEES ET GARONNE 2014-2020 »).
491

492 ## References

493 Ashe A, Colot V, Oldroyd BP. 2021. How does epigenetics influence the course of evolution? *Philosophical*
494 *Transactions of the Royal Society B: Biological Sciences* 376:20200111.

495 Baroukh C, Zemouri M, Genin S. 2022. Trophic preferences of the pathogen Ralstonia solanacearum and
496 consequences on its growth in xylem sap. *Microbiologyopen* 11:e1240.
497 Beaulaurier J, Schadt EE, Fang G. 2019. Deciphering bacterial epigenomes using modern sequencing
498 technologies. *Nat Rev Genet* 20:157–172.
499 Bergsma-Vlami M, van de Bilt JLJ, Tjou-Tam-Sin NNA, Westenberg M, Meekes ETM, Teunissen H a. S, Van
500 Vaerenbergh J. 2018. Phylogenetic Assignment of Ralstonia pseudosolanacearum (Ralstonia
501 solanacearum Phylotype I) Isolated from Rosa spp. *Plant Dis.* 102:2258–2267.
502 Blow MJ, Clark TA, Daum CG, Deutschbauer AM, Fomenkov A, Fries R, Froula J, Kang DD, Malmstrom RR,
503 Morgan RD, et al. 2016. The Epigenomic Landscape of Prokaryotes. *PLOS Genet* 12:e1005854.
504 Bourgeois JS, Anderson CE, Wang L, Modliszewski JL, Chen W, Schott BH, Devos N, Ko DC. 2022. Integration
505 of the Salmonella Typhimurium Methylome and Transcriptome Reveals That DNA Methylation
506 and Transcriptional Regulation Are Largely Decoupled under Virulence-Related Conditions. *mBio*
507 13:e0346421.
508 Casadesús J. 2016. Bacterial DNA Methylation and Methylomes. *Adv Exp Med Biol* 945:35–61.
509 Casadesús J, Low D. 2006. Epigenetic Gene Regulation in the Bacterial World. *Microbiol. Mol. Biol. Rev.*
510 70:830–856.
511 Casadesús J, Low DA. 2013. Programmed heterogeneity: epigenetic mechanisms in bacteria. *J. Biol. Chem.*
512 288:13929–13935.
513 Chapman MR, Kao CC. 1998. EpsR modulates production of extracellular polysaccharides in the bacterial
514 wilt pathogen Ralstonia (Pseudomonas) solanacearum. *J Bacteriol* 180:27–34.
515 Clark TA, Murray IA, Morgan RD, Kislyuk AO, Spittle KE, Boitano M, Fomenkov A, Roberts RJ, Korlach J.
516 2012. Characterization of DNA methyltransferase specificities using single-molecule, real-time
517 DNA sequencing. *Nucl. Acids Res.* 40:e29–e29.

518 Coupat-Goutaland B, Bernillon D, Guidot A, Prior P, Nesme X, Bertolla F. 2011. *Ralstonia solanacearum*
519 virulence increased following large interstrain gene transfers by natural transformation. *Mol.*
520 *Plant Microbe Interact.* 24:497–505.
521 Danchin E, Pocheville A, Rey O, Pujol B, Blanchet S. 2019. Epigenetically facilitated mutational assimilation:
522 epigenetics as a hub within the inclusive evolutionary synthesis. *Biol Rev Camb Philos Soc* 94:259–
523 282.
524 Davis BM, Chao MC, Waldor MK. 2013. Entering the era of bacterial epigenomics with single molecule real
525 time DNA sequencing. *Current Opinion in Microbiology* 16:192–198.
526 Ehrenreich IM, Pfennig DW. 2016. Genetic assimilation: a review of its potential proximate causes and
527 evolutionary consequences. *Ann Bot* 117:769–779.
528 Erill I, Puigvert M, Legrand L, Guarischi-Sousa R, Vandecasteele C, Setubal JC, Genin S, Guidot A, Valls M.
529 2017. Comparative analysis of Ralstonia solanacearum methylomes. *Front. Plant Sci.* [Internet] 8.
530 Available from: http://journal.frontiersin.org/article/10.3389/fpls.2017.00504/abstract
531 Estibariz I, Overmann A, Ailloud F, Krebes J, Josenhans C, Suerbaum S. 2019. The core genome m5C
532 methyltransferase JHP1050 (M.Hpy99III) plays an important role in orchestrating gene expression
533 in Helicobacter pylori. *Nucleic Acids Res* 47:2336–2348.
534 Garg RP, Huang J, Yindeeyoungyeon W, Denny TP, Schell MA. 2000. Multicomponent transcriptional
535 regulation at the complex promoter of the exopolysaccharide I biosynthetic operon of Ralstonia
536 solanacearum. *J. Bacteriol.* 182:6659–6666.
537 Gatt YE, Margalit H. 2021. Common Adaptive Strategies Underlie Within-Host Evolution of Bacterial
538 Pathogens. *Molecular Biology and Evolution* 38:1101–1121.
539 Genin S, Denny TP. 2012. Pathogenomics of the Ralstonia solanacearum species complex. *Annu Rev*
540 *Phytopathol* 50:67–89.

541 Ghosh D, Veeraraghavan B, Elangovan R, Vivekanandan P. 2020. Antibiotic Resistance and Epigenetics:
542 More to It than Meets the Eye. *Antimicrob Agents Chemother* 64:e02225-19.
543 Gopalan-Nair R, Jardinaud F, Legrand L, Lopez-Roques C, Bouchez O, Genin S, Guidot A. 2023.
544 Transcriptomic profiling reveals host-specific evolutionary pathways promoting enhanced fitness
545 in the broad host range pathogen Ralstonia pseudosolanacearum. :2023.05.12.540487. Available
546 from: https://www.biorxiv.org/content/10.1101/2023.05.12.540487v2
547 Gopalan-Nair R, Jardinaud M-F, Legrand L, Landry D, Barlet X, Lopez-Roques C, Vandecasteele C, Bouchez
548 O, Genin S, Guidot A. 2020. Convergent Rewiring of the Virulence Regulatory Network Promotes
549 Adaptation of Ralstonia solanacearum on Resistant Tomato. *Molecular Biology and Evolution*
550 38:1792–1808.
551 van der Graaf A, Wardenaar R, Neumann DA, Taudt A, Shaw RG, Jansen RC, Schmitz RJ, Colomé-Tatché M,
552 Johannes F. 2015. Rate, spectrum, and evolutionary dynamics of spontaneous epimutations.
553 *Proceedings of the National Academy of Sciences* 112:6676–6681.
554 Guidot A, Jiang W, Ferdy JB, Thébaud C, Barberis P, Gouzy J, Genin S. 2014. Multihost experimental
555 evolution of the pathogen ralstonia solanacearum unveils genes involved in adaptation to plants.
556 *Molecular Biology and Evolution* 31:2913–2928.
557 Hu J, Askary AM, Thurman TJ, Spiller DA, Palmer TM, Pringle RM, Barrett RDH. 2019. The Epigenetic
558 Signature of Colonizing New Environments in Anolis Lizards. *Mol Biol Evol* 36:2165–2170.
559 Jiang Y, Li B, Liu P, Liao F, Weng Q, Chen Q. 2016. First report of bacterial wilt caused by Ralstonia
560 solanacearum on fig trees in China. *Forest Pathology* 46:n/a-n/a.
561 Kronholm I, Bassett A, Baulcombe D, Collins S. 2017. Epigenetic and Genetic Contributions to Adaptation
562 in Chlamydomonas. *Molecular Biology and Evolution* 34:2285–2306.
563 Kronholm I, Collins S. 2016. Epigenetic mutations can both help and hinder adaptive evolution. *Mol Ecol*
564 25:1856–1868.

565 Krygier M, Podolak-Popinigis J, Limon J, Sachadyn P, Stanisławska-Sachadyn A. 2016. A simple modification
566 to improve the accuracy of methylation-sensitive restriction enzyme quantitative polymerase
567 chain reaction. *Analytical Biochemistry* 500:88–90.
568 Lefeuvre P, Cellier G, Remenant B, Chiroleu F, Prior P. 2013. Constraints on Genome Dynamics Revealed
569 from Gene Distribution among the Ralstonia solanacearum Species. *PLoS ONE* 8:e63155.
570 Lenski RE. 2017. Convergence and Divergence in a Long-Term Experiment with Bacteria. *Am Nat* 190:S57–
571 S68.
572 Lind MI, Spagopoulou F. 2018. Evolutionary consequences of epigenetic inheritance. *Heredity* 121:205–
573 209.
574 Livak KJ, Schmittgen TD. 2001. Analysis of relative gene expression data using real-time quantitative PCR
575 and the 2(-Delta Delta C(T)) Method. *Methods* 25:402–408.
576 Lopes CA, Rossato M, Boiteux LS. 2015. The Host Status Of Coffee (Coffea arabica) To Ralstonia
577 solanacearum Phylotype I Isolates. *Trop. plant pathol.* 40:1–4.
578 López-Garrido J, Casadesús J. 2010. Regulation of Salmonella enterica Pathogenicity Island 1 by DNA
579 Adenine Methylation. *Genetics* 184:637–649.
580 Macho AP, Guidot A, Barberis P, Beuzón CR, Genin S. 2010. A competitive index assay identifies several
581 Ralstonia solanacearum type III effector mutant strains with reduced fitness in host plants. *Mol.*
582 *Plant Microbe Interact.* 23:1197–1205.
583 Mayjonade B, Gouzy J, Donnadieu C, Pouilly N, Marande W, Callot C, Langlade N, Muños S. 2017.
584 Extraction of high-molecular-weight genomic DNA for long-read sequencing of single molecules.
585 *BioTechniques* 62:xv.
586 Muhammad JS, Khan NA, Maciver SK, Alharbi AM, Alfahemi H, Siddiqui R. 2022. Epigenetic-Mediated
587 Antimicrobial Resistance: Host versus Pathogen Epigenetic Alterations. *Antibiotics (Basel)* 11:809.

588 Murray IA, Clark TA, Morgan RD, Boitano M, Anton BP, Luong K, Fomenkov A, Turner SW, Korlach J,
589 Roberts RJ. 2012. The methylomes of six bacteria. *Nucl. Acids Res.* 40:11450–11462.
590 Nye TM, Jacob KM, Holley EK, Nevarez JM, Dawid S, Simmons LA, Jr MEW. 2019. DNA methylation from a
591 Type I restriction modification system influences gene expression and virulence in Streptococcus
592 pyogenes. *PLOS Pathogens* 15:e1007841.
593 Oliveira PH, Fang G. 2021. Conserved DNA Methyltransferases: A Window into Fundamental Mechanisms
594 of Epigenetic Regulation in Bacteria. *Trends in Microbiology* 29:28–40.
595 Parab L, Pal S, Dhar R. 2022. Transcription factor binding process is the primary driver of noise in gene
596 expression. *PLOS Genetics* 18:e1010535.
597 Payelleville A, Blackburn D, Lanois A, Pages S, C Cambon M, Ginibre N, Clarke DJ, Givaudan A, Brillard J.
598 2019. Role of the Photorhabdus Dam methyltransferase during interactions with its invertebrate
599 hosts. *PLoS ONE* 14:14 p.
600 Payelleville A, Brillard J. 2021. Novel Identification of Bacterial Epigenetic Regulations Would Benefit From
601 a Better Exploitation of Methylomic Data. *Front Microbiol* 12:685670.
602 Payelleville A, Legrand L, Ogier J-C, Roques C, Roulet A, Bouchez O, Mouammine A, Givaudan A, Brillard J.
603 2018. The complete methylome of an entomopathogenic bacterium reveals the existence of loci
604 with unmethylated Adenines. *Sci Rep* 8:12091.
605 Perrier A, Barlet X, Rengel D, Prior P, Poussier S, Genin S, Guidot A. 2019. Spontaneous mutations in a
606 regulatory gene induce phenotypic heterogeneity and adaptation of Ralstonia solanacearum to
607 changing environments. *Environ. Microbiol.* 21:3140–3152.
608 Perrier A, Peyraud R, Rengel D, Barlet X, Lucasson E, Gouzy J, Peeters N, Genin S, Guidot A. 2016. Enhanced
609 in planta Fitness through Adaptive Mutations in EfpR, a Dual Regulator of Virulence and Metabolic
610 Functions in the Plant Pathogen Ralstonia solanacearum. *PLOS Pathogens* 12:e1006044.

611 Plener L, Manfredi P, Valls M, Genin S. 2010. PrhG, a transcriptional regulator responding to growth
612 conditions, is involved in the control of the type III secretion system regulon in Ralstonia
613 solanacearum. *J. Bacteriol.* 192:1011–1019.
614 Ramakers C, Ruijter JM, Deprez RHL, Moorman AFM. 2003. Assumption-free analysis of quantitative real-
615 time polymerase chain reaction (PCR) data. *Neurosci. Lett.* 339:62–66.
616 Roberts RJ, Vincze T, Posfai J, Macelis D. 2015. REBASE--a database for DNA restriction and modification:
617 enzymes, genes and genomes. *Nucleic Acids Res.* 43:D298-299.
618 Sánchez-Romero MA, Casadesús J. 2020. The bacterial epigenome. *Nature Reviews Microbiology* 18:7–20.
619 Sharif J, Koseki H. 2018. Hemimethylation: DNA's lasting odd couple. *Science* 359:1102–1103.
620 Stajic D, Perfeito L, Jansen LET. 2019. Epigenetic gene silencing alters the mechanisms and rate of
621 evolutionary adaptation. *Nat Ecol Evol* 3:491–498.
622 Vailleau F, Genin S. 2023. *Ralstonia solanacearum*: An Arsenal of Virulence Strategies and Prospects for
623 Resistance. *Annu Rev Phytopathol*.
624 Valls M, Genin S, Boucher C. 2006. Integrated regulation of the type III secretion system and other
625 virulence determinants in Ralstonia solanacearum. *PLoS Pathog.* 2:e82.
626 Vandesompele J, De Preter K, Pattyn F, Poppe B, Van Roy N, De Paepe A, Speleman F. 2002. Accurate
627 normalization of real-time quantitative RT-PCR data by geometric averaging of multiple internal
628 control genes. *Genome Biol.* 3:RESEARCH0034.
629 Vogt G. 2023. Environmental Adaptation of Genetically Uniform Organisms with the Help of Epigenetic
630 Mechanisms—An Insightful Perspective on Ecoepigenetics. *Epigenomes* 7:1.
631 Walworth NG, Lee MD, Dolzhenko E, Fu F-X, Smith AD, Webb EA, Hutchins DA. 2021. Long-Term m5C
632 Methylome Dynamics Parallel Phenotypic Adaptation in the Cyanobacterium Trichodesmium. *Mol*
633 *Biol Evol* 38:927–939.

634 Weiner AKM, Katz LA. 2021. Epigenetics as Driver of Adaptation and Diversification in Microbial
635 Eukaryotes. *Front Genet* 12:642220.
636 Wicker E, Grassart L, Coranson-Beaudu R, Mian D, Guilbaud C, Fegan M, Prior P. 2007. Ralstonia
637 solanacearum strains from Martinique (French West Indies) exhibiting a new pathogenic
638 potential. *Appl. Environ. Microbiol.* 73:6790–6801.
639 Wicker E, Grassart L, Coranson-Beaudu R, Mian D, Prior P. 2009. Epidemiological evidence for the
640 emergence of a new pathogenic variant of Ralstonia solanacearum in Martinique (French West
641 Indies). *Plant Pathology* 58:853–861.
642 Wicker E, Lefeuvre P, de Cambiaire J-C, Lemaire C, Poussier S, Prior P. 2012. Contrasting recombination
643 patterns and demographic histories of the plant pathogen Ralstonia solanacearum inferred from
644 MLSA. *ISME J* 6:961–974.
645 Xue B, Sartori P, Leibler S. 2019. Environment-to-phenotype mapping and adaptation strategies in varying
646 environments. *Proceedings of the National Academy of Sciences* 116:13847–13855.
647
648

Figure legends

Figure 1 Circos plot highlighting the genomic repartition of the sites differentially methylated (DMS) between an ancestral clone and 31 clones evolved during 300 generations on five different plant species. Newly methylated sites are indicated in blue and unmethylated sites in red. A total of 31 evolved clones were investigated; 6 evolved on tomato cv. Marmande, 7 on eggplant, 3 on bean and 10 on tomato cv. Hawaii. The number of clones targeted by a DMS is indicated on the scale varying between 0 and 12 for each plant species. The black triangle indicates the position of the RSp0338 gene.

Figure 2 Relative expression level of RSp0338 gene between GMI1000 and evolved clones.

Expression level of RSp0338 was determined during growth in synthetic medium supplemented with Glutamine 10 mM at the beginning of stationary phase, using a RT-qPCR approach. The methylation profile of the GTWWAC motifs in the upstream region of epsR is indicated for each investigated clone. Three technical and three biological replicates were performed. Data were normalized using the 2-ΔΔCt calculation method (Livak and Schmittgen 2001). (Wilcoxon test, ** p value < 0,01).

Figure 3 MSRE-qPCR results for analysis of methylation status of GTWWAC motifs at the RSc2612, RSp1329 and RSp1529 genes in the ancestral GMI1000 clone.

The methylation profile of the GTWWAC motifs at the RSc2612, RSp1329 and RSp1529 genes for the ancestral GMI1000 clone was investigated using a MSRE-qPCR approach (Methylation Sensitive Restriction Enzyme- quantitative PCR). Bacterial cells were grown in synthetic medium with glutamine 10 mM and DNA was recovered at the beginning of stationary phase. The mAG4 mutant (GMI1000 deleted from the RSc1982 MTase, targeting GTWWAC motifs) was used as a non-methylated control at GTWWAC motifs. The graphs represent a relative quantification using the 2-ΔΔCt method compared to the mAG4 mutant. Detection of an amplicon revealed that no digestion occurred and that the region was

673 methylated, while non amplification revealed that the region was non-methylated and digested. 2-ΔΔCt
674 values were compared between the ancestral clone and mAG4 mutant using a Wilcoxon test; ** p-value
675 < 0.01.
676
677 **Figure 4** MSRE-qPCR results for analysis of methylation status of GTWWAC motifs upstream the RSc0102,
678 RSc0958, RSp0338, RSp0629, RSp1152 and RSp1643 genes in the ancestral GMI1000 clone and the
679 experimentally evolved clones.
680 See Figure 3 for legend. 2-ΔΔCt values were compared between the evolved or ancestral clone and mAG4
681 mutant using a Wilcoxon test; ns: not significant; ** p-value < 0.01; *** p-value < 0.001.
682
683 **Figure 5** MSRE-qPCR results for chronology of methylation appearance upstream RSp0338 during
684 experimental evolution in tomato Marmande.
685 The methylation profile of the GTWWAC motifs upstream RSp0338 was investigated using a MSRE-qPCR
686 approach for the ancestral GMI1000 clone and the ongoing experimentally evolved clones in tomato
687 Marmande host. Evolved clones in tomato Marmande from lineage B were tested at different serial
688 passaging during experimental evolution. Evolved clones are designate with MarXbx notation with X as
689 the number of serial passage experiment (SPE) and x as the clone number. See figure 4 and 3 for legend.
690
691 **Figure 6** Impact of mutation of the GTWWAC motif in the upstream region of RSp0338 gene on bacterial
692 fitness during growth into tomato var. Marmande.
693 (A) Serial passage experiments (SPE) were conducted starting with a mixed inoculum of two clones, tagged
694 with a GFP or mCherry marker, in the same proportion. At each passage, the competitive index (CI)
695 between the two clones was calculated. (B) CI values of the Mar26b2 evolved clone in competition with
696 the GMI1000 ancestral clone after 1, 2, 3 and 4 SPE. (C) CI values of the GMI1000 mutant in competition

with the GMI1000 ancestral clone after 1, 2, 3 and 4 SPE. (D) CI values of the Mar26b2 evolved clone in competition with the Mar26b2 mutant after 1, 2, 3 and 4 SPE. In brackets are indicated the methylation profiles of the GTWWAC motifs in the upstream region of the RSp0338 gene for each investigated clone and mutant. The red bar highlights CI=1. Wilcoxon test, *p-value < 0.05; **p-value < 0.01; ***p-value < 0.001.

Supplementary materials

Supplemental Figure 1 Effect of the experimental host on the number of differential methylated sites (DMSs) detected in the evolved clones according to SMRT-sequencing. A. Number of DMSs in each investigated evolved clone. B. Mean number of DMSs in evolved clones for each experimental host. Different letters above the boxplot indicate a significant difference (Wilcoxon test, p.value < 0.05). Mar: Tomato var. Marmande; Zeb : Eggplant var. Zebrina; Bean : Bean var. Blanc précoce; Cab : Cabbage var. Bartolo; Haw: Tomato var. Hawaii 7996.

Table S1 List of primers used in this study

Table S2 Genomic regions of the GMI1000 strain of Ralstonia solanacearum with a GTWWAC motif and methylation status at the beginning of the stationary phase during growth in minimal medium with glutamine 10mM

Tables

Table 1 Investigated evolved clones (derived from Gopalan-Nair et al., 2023)

Experimental host	Lineage	Evolved clone	Mean CI	Mutations		
Tomato var. Marmande	A	Mar26a1	5.6	RSc2508$^{IS, -120}$	tktA^{R326G}	RSp0128-0154$^{Del\ 33kb}$
	A	Mar26a2	5.4	RSc2508$^{IS, -120}$		
	B	Mar26b2	3.9	phcS^{T26M}		
	D	Mar26d2	5.7	RSc2508$^{IS, -120}$		
	E	Mar26e1	3.4	RSc2508$^{IS, -120}$		
	E	Mar26e3	6.3	RSc2508$^{IS, -120}$	RSp1466$^{In\ 8\ nt, -256}$	
Eggplant var. Zebrina	B	Zeb26b1	2.7	RSp0083 $^{IS, 1}$		
	B	Zeb26b5	3.7			
	C	Zeb26c2	2.1	RSp0127^{F91L}		
	C	Zeb26c3	1.6	RSp0127^{F91L}		
	C	Zeb26c4	2.1	dld^{R135S}		
	D	Zeb26d1	0.9^{ns}			
	E	Zeb26e1	3.6			
Bean var. Blanc Précoce	A	Bean26a4	6.1	RSc2508$^{A394(-)*}$	rpoB^{D428Y}	
	A	Bean26a5	6.5	RSc2508$^{A394(-)*}$		
	C	Bean26c1	6.6	efpR^{P93Q}	purF^{G-88A}	
Cabbage var. Bartolo	B	Cab36b1	4.1	RSp0955$^{IS, -1082}$	flhB $^{Dup\ 21\ nt, 1129}$	
	B	Cab36b2	4.9	RSc2508$^{IS, 760}$	RSp0955$^{IS, -1082}$	flhB $^{Dup\ 21\ nt, 1129}$
	C	Cab36c2	8.8	spoT^{A219P}	RSc2428^{C-21A}	RSc2573-2622$^{Del\ 44.4kb}$
	D	Cab36d1	3.5	phcS^{Y106C}	flgB$^{Del\ 12\ nt,483}$	RSc2573-2622$^{Del\ 44.4kb}$
	E	Cab36e3	9.4	RSc2573-2622$^{Del\ 44.4kb}$		
Tomato var. Hawaii	A	Haw35a1	8.6	soxA1^{C639R}		
	A	Haw35a4	7.2			
	B	Haw35b1	6.5	RSp1574^{V95L}		
	B	Haw35b4	12.9	RSp1574^{V95L}	prhP$^{IS, -6}$	
	C	Haw35c1	4.2			
	C	Haw35c2	4.0			
	D	Haw35d3	5.4			
	D	Haw35d5	4.1			
	E	Haw35e1	3.8	RSp1136^{C-218A}		
	E	Haw35e3	5.4	RSp1136^{C-218A}	RSc3094^{R162R}	

Note - The CI (Competitive Index) value is indicated for each evolved clone and was measured *in planta* in competition with the ancestral GMI1000 clone in our previous works (Guidot et al. 2014; Gopalan-Nair et al. 2020). In the Mutation column, the gene ID or gene name and the modification type is indicated. For SNPs inside the coding sequence, the protein modification is indicated with the original amino acid followed by the position of the SNP and by the new amino acid. For SNPs upstream the start codon of a gene, the original nucleotide is indicated followed by the position of the SNP from the start codon and by the new nucleotide. For small insertion (In), deletion (Del) and duplication (Dup), the size of the modification is indicated followed by the position of the modification. For IS insertion (IS), the position of the insertion is indicated upstream the start codon or in the coding sequence of the gene. *Single nucleotide deletion; ns, not significantly different from the ancestral clone; nt, nuclotides.

Table 2 Genomic regions of the GMI1000 strain of *Ralstonia solanacearum* with a GTWWAC motif detected unmethylated or hemimethylated at the beginning of the stationary phase during growth in synthetic medium with glutamine 10mM according to SMRT-seq data

Replicon	Gene ID	Gene name	Gene Description	position strand -	position strand +	Motif	upstream, intragenic*	methylation status**
								SMRT-seq
Chromosome	RSc0958		type VI secretion system tip VgrG family protein	1004576	1004579	GTTAAC	upstream	unmethylated
Chromosome	RSc2561		Conserved protein, DUF3313 domain-containing	2769503	2769506	GTTTAC	upstream	unmethylated
Chromosome	RSc2612		ICE Tn4371 - Hypothetical protein	2813720	2813723	GTTTAC	intragenic	unmethylated
Chromosome	RSc3132		Transcription regulator, XRE family with a cupin C-terminal domain	3378821	3378824	GTTTAC	upstream	unmethylated
Megaplasmid	RSp0338	*epsR*	Negative regulator of EPS production EpsR, Transcription regulator, NarL/FixJ family	445723	445726	GTTTAC	upstream	unmethylated
Megaplasmid	RSp0338	*epsR*	Negative regulator of EPS production EpsR, Transcription regulator, NarL/FixJ family	445735	445738	GTAAAC	upstream	unmethylated
Megaplasmid	RSp0629		Type VI secretion system tip VgrG family protein with DUF2345 domain	765405	765408	GTTAAC	upstream	unmethylated
Megaplasmid	RSp1329		hypothetical protein	1680220	1680223	GTATAC	intragenic	unmethylated
Megaplasmid	RSp1398/RSp1399	*aroE2/*	shikimate 5-dehydrogenase/porin	1761411	1761414	GTAAAC	upstream	unmethylated
Megaplasmid	RSp1529	*efe*	1-aminocyclopropane-1-carboxylate oxidase (Ethylene-forming enzyme)	1916009	1916012	GTTTAC	upstream	unmethylated
Chromosome	RSc0081		Transcription regulator, MurR/RpiR family	94117	94120	GTTAAC	upstream	hemimethylated strand +
Chromosome	RSc0608	*ripAA*	type III effector protein RipAA	655714	655717	GTTAAC	upstream	hemimethylated strand +
Chromosome	RSc2094/RSc2095	*xanR/xdhA*	Purine salvage pathway regulator XanR, Transcription Regulator, LysR family/Xanthine Dehydrogenase, subunit A	2267247	2267250	GTTTAC	upstream	hemimethylated strand +
Megaplasmid	RSp1025		Translocator, LysE family	1298046	1298049	GTTTAC	upstream	hemimethylated strand +
Chromosome	RSc2176	*tISRso5*	ISRSO5-transposase protein	2360129	2360132	GTTAAC	upstream	hemimethylated strand -
Chromosome	RSc2176	*tISRso5*	ISRSO5-transposase protein	2360143	2360146	GTAAAC	upstream	hemimethylated strand -
Megaplasmid	RSp0216/RSp0217	*/ tISRso5*	Pseudogene: Type 3 Secretion effector RipBM (C-terminal fragment)/ ISRSO5-transposase protein	269725	269728	GTTAAC	intragenic / upstream	hemimethylated strand -
Megaplasmid	RSp1544		hypothetical protein	1939052	1939055	GTAAAC	intragenic	hemimethylated strand -
Megaplasmid	RSp1675	*tISRso5*	ISRSO5-transposase protein	2087332	2087335	GTTAAC	upstream	hemimethylated strand -

Note - Raw data from SMRT-seq analysis are given in Table S2. *GTWWAC motifs were annotated intragenic if their positions mapped within the annotated coding sequence and upstream if they mapped to the first non-coding 300 bp before the annotated start codon. **for hemimethylated motifs, the strand which is not methylated is indicated.

Table 3a Differential methylated sites on the chromosome between the ancestral clone and the clones evolved on five different plant species

Gene ID	Motif	upstream / inside the ORF	*Gene name*	Gene function	Position	Ancestral clone	Tomato var. Marmande						Eggplant var. Zebrina							Bean var. BP			Cabbage var. Bartolo					Tomato var. Hawaii 7996									
						GMI1000 methylation profil	a1	a2	b2	d2	e1	e3	b1	b5	c2	c3	c4	d1	e1	a4	a5	c1	b1	b2	c2	d1	e3	a1	a4	b1	b4	c1	c2	d3	d5	e1	e3
RSc0081	GTTAAC	upstream		Transcriptional regulator, MurR/RpiR family	94117	6mA					6A							6A							6A								6A		6A		
RSc0081	GTTAAC	upstream		Transcriptional regulator, MurR/RpiR family	94120	6A		6mA	6mA	6mA	6mA	6mA	6mA	6mA	6mA	6mA	6mA	6mA				6mA	6mA	6mA	6mA		6mA	6mA	6mA	6mA	6mA		6mA			6mA	6mA
RSc0102 / RSc0103	GTTAAC	upstream	*/ tISRso5*	Pseudogene: Ca2+-binding protein, RTX toxin-related (C-terminal fragment) / Transposase (ISRSO5 family)	117936	6mA																										6A		6A		
RSc0102 / RSc0103	GTTAAC	upstream	*/ tISRso5*	Pseudogene: Ca2+-binding protein, RTX toxin-related (C-terminal fragment) / Transposase (ISRSO5 family)	117939	6mA																										6A				
RSc0102 / RSc0103	GTAAAC	upstream	*/ tISRso5*	Pseudogene: Ca2+-binding protein, RTX toxin-related (C-terminal fragment) / Transposase (ISRSO5 family)	117950	6mA														6A																	
RSc0109 / RSc0110	GTTAAC	upstream	*thiG / tISRso5*	Thiazole synthase ThiG / Transposase (ISRSO5 family)	127847	6mA												6A																		
RSc0608	GTTAAC	upstream	*ripAA*	Type III effector protein RipAA	655714	6mA								6A										6A										6A	6A	
RSc0608	GTTAAC	upstream	*ripAA*	Type III effector protein RipAA	655717	6A	6mA	6mA	6mA	6mA	6mA	6mA	6mA	6mA	6mA	6mA	6mA	6mA	6mA	6mA	6mA	6mA	6mA	6mA	6mA	6mA	6mA	6mA	6mA	6mA	6mA	6mA	6mA	6mA		6mA	6mA
RSc0637	GTTAAC	upstream	*tISRso5*	ISRSO5-transposase protein	683376	6mA																										6A		6A		
RSc0637	GTTAAC	upstream	*tISRso5*	Transposase (ISRSO5 family)	683379	6mA																											6A				
RSc0958	GTTAAC	upstream		Type VI secretion system tip VgrG family protein	1004576	6A																	6mA		6mA								6mA				
RSc0958	GTTAAC	upstream		Type VI secretion system tip VgrG family protein	1004579	6A					6mA				6mA	6mA	6mA	6mA			6mA		6mA	6mA									6mA			6mA	
RSc1078 / RSc1079	GTAAAC	upstream	*/gudD1*	Transcription regulator / D-Glucarate dehydratase	1134729	6mA														6A																
RS06160	GTAAAC	intragenic		Ribosomal RNA-23S	1202810	6mA														6A																
RSc1539	GTATAC	upstream	*sixA*	Phosphohistidine phosphatase SixA	1645829	6mA														6A																
RSc2095	GTTAAC	upstream	*xdhA*	Xanthine Dehydrogenase, subunit A	2267250	6A	6mA	6mA	6mA	6mA	6mA	6mA	6mA	6mA	6mA	6mA	6mA	6mA	6mA	6mA	6mA	6mA	6mA	6mA	6mA	6mA	6mA	6mA	6mA	6mA	6mA	6mA	6mA	6mA	6mA	6mA	6mA	6mA
RSc2176	GTAAAC	upstream	*tISrso5*	ISRSO5-transposase protein	2360129	6A	6mA	6mA	6mA	6mA	6mA	6mA	6mA	6mA	6mA	6mA	6mA	6mA	6mA	6mA	6mA	6mA	6mA	6mA	6mA	6mA	6mA	6mA	6mA	6mA	6mA	6mA	6mA	6mA	6mA	6mA	6mA	6mA
RSc2176	GTAAAC	upstream	*tISrso5*	ISRSO5-transposase protein	2360143	6A	6mA	6mA	6mA	6mA	6mA	6mA	6mA	6mA	6mA	6mA	6mA	6mA	6mA	6mA	6mA	6mA	6mA	6mA	6mA	6mA	6mA	6mA	6mA	6mA	6mA	6mA	6mA	6mA	6mA	6mA	6mA	6mA
RSc2490 / RSc2492	GTTAAC	upstream	*icd/*	Isocitrate dehydrogenase / Acid phosphatase	2697793	6mA														6A																
RSc2534	GTAAAC	upstream		Oxidoreductase	2741386	6mA								6A																						
RSc2612	GTAAAC	intragenic		ICE Tn4371 - Hypothetical protein	2813720	6A	6mA	6mA	6mA	6mA	6mA	6mA	6mA	6mA	6mA	6mA	6mA	6mA	6mA	6mA	6mA	6mA	6mA	6mA					6mA	6mA	6mA	6mA	6mA	6mA	6mA	6mA	6mA	6mA
RSc2612	GTAAAC	intragenic		ICE Tn4371 - Hypothetical protein	2813723	6A	6mA	6mA	6mA	6mA	6mA	6mA	6mA	6mA	6mA	6mA	6mA	6mA	6mA	6mA	6mA	6mA	6mA	6mA						6mA	6mA	6mA	6mA	6mA	6mA	6mA	6mA		6mA
RSc2654	GTAAAC	upstream		Peptidase, S8 family	2856885	6mA	6A			6A	6A								6A	6A	6A		6A			6A							6A		6A		
RSc2918	GTAAAC	upstream		RNA polymerase sigma factor, RpoE family protein	3145217	6mA													6A																		
RSc3177	GTTAAC	upstream		Cyclic nucleotide binding domain-containing protein	3435906	6mA			6A	6A		6A							6A	6A		6A	6A		6A	6A				6A		6A	6A			6A	
RSc3393	GTTAAC	upstream	*tISRso5*	Transposase (ISRSO5 family)	3660531	6mA								6A																						

Note - GTWWAC motifs were annotated intragenic if their positions mapped within the annotated coding sequence and upstream if they mapped to the first non-coding 300 bp before the annotated start codon. In grey boxes are indicated the two strand differential methylated sites. The DMSs investigated by MSRE-qPCR are boxed. BP : Blanc Précoce; EPS : exopolysaccharides

Table 3b Differential methylated sites on the megaplasmid between the ancestral clone and the clones evolved on five different plant species

Gene ID	Motif	upstream / inside the ORF	*Gene name*	Gene function	Position	Ancestral clone	Tomato var. Marmande						Eggplant var. Zebrina							Bean var. BP			Cabbage var. Bartolo				Tomato var. Hawaii 7996									
						GMI1000 methylation profil	a1	a2	b2	d2	e1	e3	b1	b5	c2	c3	c4	d1	e1	a4	a5	c1	b1	b2	c2	d1	e3	a1	a4	b1	b4	c1	c2	d3	d5	e1	e3
RSp0077	GTTAAC	upstream		Type II toxin-antitoxin system, RelE/ParE toxin family	87279	6mA																							6A	6A						
RSp0216 / RSp0217	GTTTAC	intragenic / upstream	*/tISRso5*	Pseudogene: Type 3 Secretion effector RipBM (C-terminal fragment) / ISRSO5-transposase protein	269725	6A	6mA	6mA	6mA	6mA	6mA	6mA	6mA	6mA	6mA	6mA	6mA	6mA	6mA	6mA	6mA	6mA	6mA	6mA	6mA	6mA	6mA	6mA	6mA	6mA	6mA	6mA	6mA	6mA	6mA	6mA
RSp0338	GTTTAC	upstream	*epsR*	Transcription Regulator EpsR	445723	6A			6mA												6mA						6mA										
RSp0338	GTAAAC	upstream	*epsR*	Transcription Regulator EpsR	445726	6A			6mA												6mA						6mA										
RSp0338	GTAAAC	upstream	*epsR*	Transcription Regulator EpsR	445735	6A			6mA																		6mA										
RSp0338	GTTTAC	upstream	*epsR*	Transcription Regulator EpsR	445738	6A			6mA												6mA						6mA										
RSp0449	GTAAAC	intragenic		Pseudogene: RSH repeat protein (C-terminal fragment)	561449	6mA														6A																	
RSp0454	GTTAAC	intragenic		Pseudogene: RHS repeat protein (N-terminal fragment)	565511	6mA																														6A	
RSp0629	GTTAAC	upstream		Type 6 secretion system tip VgrG family protein with DUF2345 domain	765405	6A		6mA															6mA				6mA										
RSp0629	GTTAAC	upstream		Type 6 secretion system tip VgrG family protein with DUF2345 domain	765408	6A																	6mA				6mA										
RSp0641	GTAAAC	intragenic	*rmyB*	Ralsolamycin synthase, unit B	792207	6mA													6A																		
RSp0726	GTAAAC	intragenic		Major facilitator superfamily (MFS) transporter	913370	6mA														6A																		
RSp1025	GTTTAC	upstream		Translocator, LysE family	1298049	6A	6mA	6mA	6mA	6mA	6mA	6mA	6mA	6mA	6mA	6mA	6mA	6mA		6mA	6mA	6mA	6mA	6mA		6mA	6mA	6mA	6mA	6mA	6mA	6mA	6mA	6mA	6mA	6mA	6mA	6mA
RSp1152	GTTAAC	upstream	*tISRso5*	Transposase (ISRSO5 family)	1452556	6mA												6A													6A						
RSp1152	GTTAAC	upstream	*tISRso5*	Transposase (ISRSO5 family)	1452559	6mA																									6A						
RSp1329	GTATAC	intragenic		hypothetical protein	1680220	6A	6mA		6mA	6mA	6mA	6mA	6mA	6mA	6mA	6mA	6mA	6mA	6mA	6mA	6mA	6mA	6mA	6mA	6mA	6mA	6mA		6mA	6mA			6mA	6mA			6mA	6mA
RSp1329	GTATAC	intragenic		hypothetical protein	1680223	6A	6mA	6mA	6mA	6mA	6mA	6mA	6mA	6mA	6mA	6mA	6mA	6mA	6mA	6mA	6mA	6mA		6mA		6mA	6mA	6mA		6mA								6mA	6mA
RSp1529	GTAAAC	upstream	*efe*	1-aminocyclopropane-1-carboxylate oxidase (Ethylene-forming enzyme)	1916009	6A	6mA	6mA	6mA	6mA	6mA	6mA	6mA		6mA	6mA	6mA		6mA	6mA	6mA	6mA	6mA	6mA	6mA		6mA	6mA	6mA	6mA	6mA	6mA	6mA			6mA	6mA
RSp1529	GTAAAC	upstream	*efe*	1-aminocyclopropane-1-carboxylate oxidase (Ethylene-forming enzyme)	1916012	6A				6mA																6mA											
RSp1544	GTTAAC	intragenic		hypothetical protein	1939052	6A	6mA		6mA	6mA		6mA	6mA	6mA	6mA	6mA		6mA	6mA	6mA	6mA			6mA	6mA	6mA		6mA	6mA	6mA	6mA	6mA	6mA	6mA				6mA
RSp1545	GTAAAC	intragenic		Filamentous hemagglutinin family protein	1939296	6mA																									6A						
RSp1643	GTTAAC	upstream		Hypothetical protein	2062924	6mA															6A									6A						
RSp1643	GTTAAC	upstream		Hypothetical protein	2062927	6mA																								6A				6A		
RSp1675	GTTAAC	upstream	*tISRso5*	ISRSO5-transposase protein	2087332	6A	6mA	6mA	6mA	6mA	6mA	6mA	6mA	6mA	6mA	6mA	6mA	6mA	6mA	6mA	6mA	6mA	6mA	6mA	6mA	6mA	6mA	6mA	6mA	6mA	6mA	6mA	6mA	6mA	6mA	6mA	6mA

Note - GTWWAC motifs were annotated intragenic if their positions mapped within the annotated coding sequence, upstream if they mapped to the first non-coding 300 bp before the annotated start codon. In grey boxes are indicated the two strand differential methylated sites. The DMSs investigated by MSRE-qPCR are boxed. BP : Blanc Précoce; EPS : exopolysaccharides.

748 **Table 4** General features of the differential methylated sites (DMSs) identified in evolved clones from five different plant species

	Genome (5.8 Mbp)	Chromosome (3.7 Mbp)	Megaplamsid (2.1 Mbp)
nbr of DMSs	**50**	**26**	**24**
DMS frequency / Mbp	*8,62*	*7,03*	*11,43*
nbr of genes affected by DMSs	**39**	**22**	**17**
nbr of DMSs in gene promoter region	**39**	**23**	**16**
% DMSs in gene promoter regions	*78*	*88*	*67*
nbr of DMSs affecting transposable elements	**13**	**9**	**4**
% transposable elements/nbr of DMSs in gene promoter regions	*33*	*39*	*25*
nbr of DMSs affecting virulence determinants	**12**	**4**	**8**
% virulence determinants/nbr of DMSs in gene promoter regions	*31*	*17*	*50*

749

750 Note - *Gene promoter region was defined as the first non-coding 300 bp region before the annotated start codon of the gene. Mbp : million of base pairs

751

752 **Table 5a** Relative gene expression in the experimentally evolved clone compared to the ancestral clone for each gene targetted by a differential

753 methylated site

754

Gene ID	Tomato var. Marmande						Eggplant var. Zebrina							Bean var. BP			Cabbage var. Bartolo					Tomato var. Hawaii 7996									
	a1	a2	b2	d2	e1	e3	b1	b5	c2	c3	c4	d1	e1	a4	a5	c1	b1	b2	c2	d1	e3	a1	a4	b1	b4	c1	c2	d3	d5	e1	e3
RSc0081	0,24	0,03	-2,40	0,41	0,23	-0,26	-1,12	0,35	-0,23	0,81	0,25	-0,13	-0,40	-2,25	-2,33	-0,76	-0,39	-0,91	-1,09	-0,09	-0,58	-0,52	-0,49	0,51	-0,19	-0,24	-0,47	0,13	0,78	0,47	0,44
RSc0102	4,65	4,71	5,88	3,95	3,12	4,37	0,34	-0,48	0,08	-0,55	-0,35	0,56	0,59	0,43	0,26	1,13	4,85	4,23	4,51	5,74	4,45	1,53	0,29	0,26	0,92	0,86	0,31	-0,21	-0,59	-0,31	-0,72
RSc0103	-0,70	-0,78	0,29	-1,98	-2,88	-1,75	0,22	0,81	0,44	0,22	0,15	1,09	-0,22	-0,45	-0,03	1,38	-0,95	-1,49	-1,19	-0,10	-1,33	0,53	-0,15	0,27	0,40	0,87	0,24	0,03	0,06	-0,41	-0,71
RSc0109	-0,29	-0,38	-2,07	0,54	0,97	0,05	-1,30	-0,24	-0,92	0,75	-0,85	-1,08	0,41	0,30	0,70	0,17	-0,19	-0,67	-1,48	-0,20	-0,21	0,14	-0,72	-0,11	-0,44	-0,07	-0,53	-0,26	0,21	0,23	-0,04
RSc0110	1,46	1,21	-0,38	1,48	0,32	1,55	0,57	0,64	0,54	-0,10	0,46	0,36	-0,52	-0,52	-0,26	0,66	1,63	1,33	1,60	1,59	1,92	0,42	0,56	0,72	0,56	1,61	1,56	1,41	1,26	1,93	1,63
RSc0608	-0,07	0,30	0,40	0,84	-0,14	0,55	-0,30	0,32	-0,52	-0,43	-0,34	0,14	0,81	0,01	-0,39	-2,02	1,52	-0,01	-0,92	-1,47	0,73	-0,15	0,06	-1,76	-1,51	-2,79	-2,34	-0,81	-0,85	-1,02	-1,38
RSc0637	-1,60	-1,30	-0,20	-1,87	-2,52	-1,75	-0,19	-0,54	0,48	-0,75	-0,88	0,29	-0,69	-0,60	-0,77	-0,53	-1,24	-1,35	-0,70	-0,39	-1,59	-0,56	-0,07	-0,52	-0,71	-0,60	-0,25	-1,37	-0,88	-1,27	-1,15
RSc0958	-0,27	-0,12	0,67	-0,36	-0,32	-0,10	0,24	0,04	0,40	-0,18	0,14	0,43	0,24	0,51	0,51	0,35	-0,05	0,28	0,64	0,08	0,04	0,22	0,44	-0,02	0,49	0,14	0,25	0,04	-0,21	-0,32	-0,17
RSc1078	3,31	2,85	0,76	3,61	3,03	2,91	0,10	0,51	-0,15	0,40	0,80	-0,34	0,66	0,49	0,53	-0,61	2,62	1,94	1,80	3,29	2,96	-0,14	-0,66	0,40	0,05	0,09	0,13	0,28	-0,11	0,26	0,81
RSc1079	0,05	-0,21	-1,32	0,15	-0,98	0,22	-0,79	0,23	-0,42	0,38	-0,21	-0,39	0,40	-1,08	-1,29	-0,13	0,30	-0,01	-0,91	0,62	0,30	-0,09	-0,52	-0,13	-0,21	0,37	-0,08	0,06	0,21	-0,17	0,06
RSc1539	0,16	0,19	-0,40	0,55	-0,12	0,27	-0,23	0,37	-0,57	-0,99	-0,05	-1,49	0,64	-0,34	-0,96	-0,45	0,40	-0,36	-0,77	0,70	-0,40	0,05	0,03	-0,06	0,04	-0,03	0,12	-0,41	0,30	0,50	0,52
RSc2095	0,89	0,40	-0,10	0,27	0,63	0,41	0,43	0,57	0,55	0,36	0,64	0,54	0,28	0,82	0,30	0,30	0,66	-0,31	0,57	1,43	0,41	0,90	0,45	0,73	0,59	1,30	0,67	0,63	0,58	0,62	0,55
RSc2176	-1,82	-1,40	-0,08	-2,26	-2,63	-1,72	0,10	-0,75	-0,26	-0,75	-0,64	-0,22	-1,29	-0,43	-0,30	-0,63	-2,31	-1,78	-0,53	-2,10	-1,49	-0,58	-0,08	-1,23	-1,00	-1,18	-0,88	-0,92	-1,00	-1,18	-1,13
RSc2490	-0,60	-0,30	-0,05	-0,10	-0,19	0,12	0,13	0,28	0,57	0,01	0,46	0,56	-0,31	1,00	0,80	0,26	-0,03	0,85	-0,13	-0,63	-0,02	-0,03	-0,01	-0,49	-0,61	-0,32	-0,03	-0,07	-0,24	-0,23	-0,38
RSc2491	0,32	0,28	0,96	-0,70	-0,34	0,05	-0,03	0,15	-0,17	-0,03	-0,94	0,93	1,00	0,60	0,03	-0,04	0,56	1,23	1,01	-0,35	0,40	0,95	0,90	0,41	0,11	-0,18	0,87	1,09	0,81	0,76	0,79
RSc2492	0,26	-0,14	-1,30	-0,37	-0,63	-0,22	-0,33	-0,57	-0,40	0,05	-0,34	-0,45	0,22	-0,25	-0,64	-0,26	-0,53	-0,95	-0,34	-0,03	-0,10	-0,20	-0,31	-0,04	-0,19	-0,02	-0,29	-0,57	-0,15	-0,15	-0,30
RSc2534	1,23	0,66	-1,02	1,00	-0,24	-0,19	-1,53	0,58	-0,37	0,93	0,20	-0,09	1,09	-0,44	-0,32	-0,30	0,61	-1,12	-2,07	2,07	-0,33	0,78	-0,46	0,42	-0,91	1,27	-0,50	0,20	0,35	0,76	0,68
RSc2612	-1,28	-0,75	0,78	-1,31	-0,70	-1,50	-0,35	-0,51	-0,16	-0,37	-0,38	0,59	-0,45	0,45	0,71	0,67	-0,60	0,87	na	na	na	-0,52	-0,10	-1,27	-0,72	-0,46	-0,17	-0,50	-0,65	-1,29	-1,15
RSc2654	-0,29	-0,40	0,33	-0,36	0,08	-0,38	-0,12	-0,08	-0,30	-0,05	-0,27	-0,02	-0,63	0,01	0,04	-0,01	-0,03	0,02	0,09	-0,29	-0,46	-0,29	0,04	0,31	0,03	-0,03	0,24	0,02	0,10	-0,03	0,03
RSc2918	0,14	0,12	-1,15	-0,03	0,81	-0,16	0,08	-0,22	-0,32	-0,02	0,42	0,01	-0,59	1,19	1,58	0,15	-0,42	0,89	0,45	-0,90	-0,02	0,36	0,37	0,68	0,50	0,24	-0,01	0,48	0,51	0,42	0,31
RSc3177	1,36	1,22	2,51	0,50	-0,90	0,73	0,72	1,37	0,70	0,50	0,66	1,39	1,03	-0,21	0,01	1,68	2,07	0,37	1,48	2,41	0,87	2,19	1,22	1,19	1,63	1,95	0,92	1,07	0,80	0,66	0,66
RSc3393	4,82	5,41	5,86	3,93	2,54	4,40	-1,13	-1,74	-0,03	-0,81	-1,23	-0,22	-0,67	-1,21	-1,24	-0,68	4,47	4,57	4,50	5,43	4,91	0,02	0,11	-0,88	-0,81	0,00	-0,05	-0,59	-1,25	-1,44	-0,60
RSp0077	0,56	0,22	0,60	-0,67	-2,18	-0,06	-0,32	-0,07	0,18	-0,43	0,02	0,20	-0,13	-1,91	-1,09	0,42	0,34	-1,07	-0,13	1,42	0,15	0,51	0,10	0,05	-0,19	0,78	0,43	0,00	0,11	-0,43	0,18
RSp0216	0,14	0,40	2,19	-0,16	0,61	0,04	0,09	-0,26	0,41	-0,53	-0,16	0,50	0,21	1,07	0,57	0,55	0,51	0,98	0,95	0,92	0,71	0,94	0,36	0,01	0,12	0,57	0,28	-0,12	-0,45	-0,49	-0,40
RSp0217	-0,12	-0,15	0,97	-0,97	-0,54	-0,74	-0,04	-0,37	-0,01	-0,96	-0,39	-0,14	-1,19	-1,20	-1,11	-0,54	-0,37	-0,10	0,60	0,42	-0,60	-0,65	-0,25	-0,86	-0,84	-1,13	-0,80	-1,13	-0,74	-1,18	-1,15
RSp0338	-0,56	0,00	-1,27	-1,03	-0,23	-0,67	0,04	-0,39	0,51	0,07	0,23	0,58	-0,48	0,33	0,40	-0,84	-0,71	0,70	0,09	-2,89	-0,36	-1,67	0,21	-1,10	-0,99	-1,28	0,02	-0,08	-0,08	-0,24	-0,51
RSp0449	-0,19	-0,15	1,67	-0,91	-1,95	-0,60	-0,06	-0,45	-0,14	-0,60	-0,51	0,37	0,19	-1,52	-1,61	0,16	0,29	-0,61	0,84	1,32	-0,07	0,33	0,59	-0,48	0,60	-0,03	-0,03	-0,25	-0,59	-0,75	-0,75
RSp0454	-0,73	-0,43	1,69	-1,10	-0,63	0,04	0,55	-1,07	-0,16	-1,33	-0,43	-0,87	0,08	0,51	0,03	0,21	-0,28	-0,18	0,59	0,25	0,34	0,98	0,57	-0,47	0,48	0,09	-0,38	-0,91	-1,13	-0,92	-1,08
RSp0629	0,62	0,68	1,28	0,43	1,18	0,66	0,50	-0,35	0,15	-0,26	-0,12	0,05	0,32	1,87	1,72	0,25	0,35	1,41	1,22	0,65	0,95	0,54	0,17	0,46	0,69	0,43	0,19	-0,11	-0,23	0,05	-0,14
RSp0641	0,36	0,42	0,87	1,25	0,98	1,75	0,79	1,36	0,54	0,20	0,39	0,15	1,83	1,39	1,32	1,50	1,48	0,94	0,22	-1,10	1,14	1,51	0,31	1,02	1,78	1,58	0,12	0,31	0,43	0,52	0,85
RSp0726	0,21	0,95	2,27	-0,17	-0,20	0,12	-0,01	-0,33	0,22	-0,48	-0,22	0,35	0,29	0,42	0,53	0,43	0,49	0,73	1,51	0,26	0,46	0,58	0,31	-0,03	0,31	0,43	0,22	-0,27	-0,35	-0,54	-0,42
RSp1025	-1,35	-1,19	-0,68	-0,86	-0,68	-1,27	0,75	0,21	0,02	-0,20	-0,05	0,30	-0,79	-0,38	-0,49	-0,80	-1,38	-0,70	-0,03	-3,49	-1,29	-0,78	0,36	-0,98	-1,85	-1,75	-1,04	-0,31	-0,38	-0,25	-0,54
RSp1152	-0,53	-0,47	0,15	-1,65	-2,47	-1,24	-0,48	0,13	0,27	0,02	0,17	0,51	0,13	-1,04	-0,82	0,38	-0,76	-1,79	-0,45	0,14	-1,72	0,61	0,02	0,06	0,23	0,39	-0,27	-0,38	-0,14	-0,73	-1,06
RSp1329	na	na	na	na	na	na	na	na	na	na	na	na	na	na	na	na	na	na	na	na	na	na	na	na	na	na	na	na	na	na	na
RSp1529	1,04	1,11	1,75	0,44	-0,30	0,65	0,09	-0,39	0,05	-0,74	-0,44	-0,15	-0,31	0,00	-0,10	-0,19	1,91	0,41	2,70	0,95	0,74	0,42	0,28	0,19	0,10	-0,03	-0,20	-0,30	-0,89	-0,40	-0,22
RSp1544	-1,65	-1,38	1,50	-2,35	-2,48	-2,06	-0,18	-0,18	-0,08	-0,31	-0,41	0,74	-0,53	-0,86	-0,90	0,12	-0,92	-1,18	0,27	-0,35	-1,58	-0,18	0,42	-0,92	0,28	-0,66	-0,53	-0,83	-1,11	-1,65	-1,48
RSp1545	-0,12	-0,14	0,77	-0,69	-1,05	-0,53	-0,34	-0,70	-0,22	-0,57	-0,78	0,40	-0,40	-1,04	-1,07	-0,20	-0,19	-0,41	0,29	0,44	-0,24	-0,31	0,17	-0,55	0,13	-0,35	-0,50	-0,66	-0,81	-1,28	-1,02
RSp1643	1,00	1,46	1,63	0,63	0,60	1,23	0,45	-0,27	0,05	-0,45	-1,21	0,02	0,90	0,13	0,53	-0,45	1,39	1,56	1,51	1,36	1,39	-0,97	0,18	1,11	1,87	-0,79	-0,20	-0,29	-0,57	-0,67	-0,46
RSp1675	0,44	0,63	1,54	-0,35	-0,93	0,10	-0,73	-1,04	0,22	-0,81	-0,63	0,30	-0,71	-1,99	-1,20	-0,32	0,60	-0,19	0,85	1,23	0,06	-0,05	-0,10	-0,70	-0,84	-1,00	-0,10	-0,96	-1,17	-1,38	-1,06

Note - RNAseq analyis was conducted with RNA extracted from bacterial cultures in synthetic medium with 10 mM Glutamine at the beginning of stationary phase. The table gives the log Fold change values. RNAseq raw data and analysis are given in Gopalan-Nair et al. (2023). In green are the downregulated genes and in yellow the upregulated genes (I logFC I > 0.5; p-value < 0.05; FDR < 0.08). The values in red indicate the clone in which the gene was targetted by a differential methylated site (Table 3). na : non available data; in the Cab36c2, d1 and e3 clones, the RSc2612 gene is deleted (see Table 1).

Table 5b Association analysis between differential methylation and differential gene expression between the ancestral clone and the experimentally evolved clones

Gene ID	DMS-DEG	DMS-non DEG	non DMS-DEG	non DMS-non DEG	*p*- value (Fisher exact Test)
RSc0081	0	4	10	17	0,2770
RSc0102	2	1	15	13	1,0000
RSc0103	1	2	10	18	1,0000
RSc0109	1	0	6	24	0,2258
RSc0110	0	1	16	14	0,4839
RSc0608	3	1	9	18	0,2718
RSc0637	1	2	12	16	1,0000
RSc0958	2	8	2	19	0,5773
RSc1078	0	1	10	20	1,0000
RSc1079	1	0	7	23	0,2581
RSc1539	0	1	0	30	1,0000
RSc2095	13	18	0	0	1,0000
RSc2176	20	11	0	0	1,0000
RSc2490	1	0	5	25	0,1935
RSc2491	0	1	13	17	1,0000
RSc2492	1	0	3	27	0,1290
RSc2534	0	1	11	19	1,0000
RSc2612	7	21	0	0	1,0000
RSc2654	1	9	0	21	0,3226
RSc2918	0	1	4	26	1,0000
RSc3177	11	2	12	6	0,4120
RSc3393	0	1	12	18	1,0000
RSp0077	1	1	5	24	0,3548
RSp0216	8	23	0	0	1,0000
RSp0217	17	14	0	0	1,0000
RSp0338	3	0	5	23	0,0125
RSp0449	1	0	11	19	0,3871
RSp0454	1	0	11	19	0,3871
RSp0629	3	0	10	18	0,0636
RSp0641	1	0	18	12	1,0000
RSp0726	1	0	6	24	0,2258
RSp1025	15	14	0	2	0.4839
RSp1152	0	2	10	19	1,0000
RSp1329	na	na	na	na	na
RSp1529	1	1	9	20	1,0000
RSp1544	12	11	6	2	0.412
RSp1545	0	1	15	15	1,0000
RSp1643	1	1	11	18	1,0000
RSp1675	11	20	0	0	1,0000

Note - For each gene targetted by a differentially methylated site (DMS) in at least one experimentaly evolved clone, the table gives the number of clones in which the gene is both differentially methylated and differentially expressed (DMS-DEG (Differentially espressed gene)), differentially methylated but not differentially expressed (DMS-non DEG), not differentially methylated but differentially expressed (non DMS-DEG) and neither differentially methylated nor expressed (non DMS - non DEG). A fisher exact test was used to determine whether there was an association between methylation and gene expression.

770 **Table 6** Methylation profiles of GMI1000 and Mar26b2 clones and their corresponding epsR-GTWWAC
771 mutants at the beginning of the stationnary phase during growth in synthetic medium with glutamine 10
772 mM.

Gene ID	Motifs	Mutations	DNA strand	Methylation profile			
				GMI1000	GM1000 mutant	Mar26b2	Mar26b2 mutant
epsR	GTAAACAAAAAGGTTTAC	GCAAACAAAAAGGCTTAC	+	6A6A	6A6A	6mA6mA	6A6A
	CATTTGTTTTTCCAAATG	CGTTTGTTTTTCCGAATG	-	6A6A	6A6A	6mA6mA	6A6A

773

774

Figure 1


Position (kb)
Repeat regions
Genes
Eggplant
Bean
Tomato cv. Hawaii
Tomato cv. Marmande
Cabbage
Methylated
Unmethylated
RSp0338 (epsR)
Megaplasmid
Chromosome

Figure 2

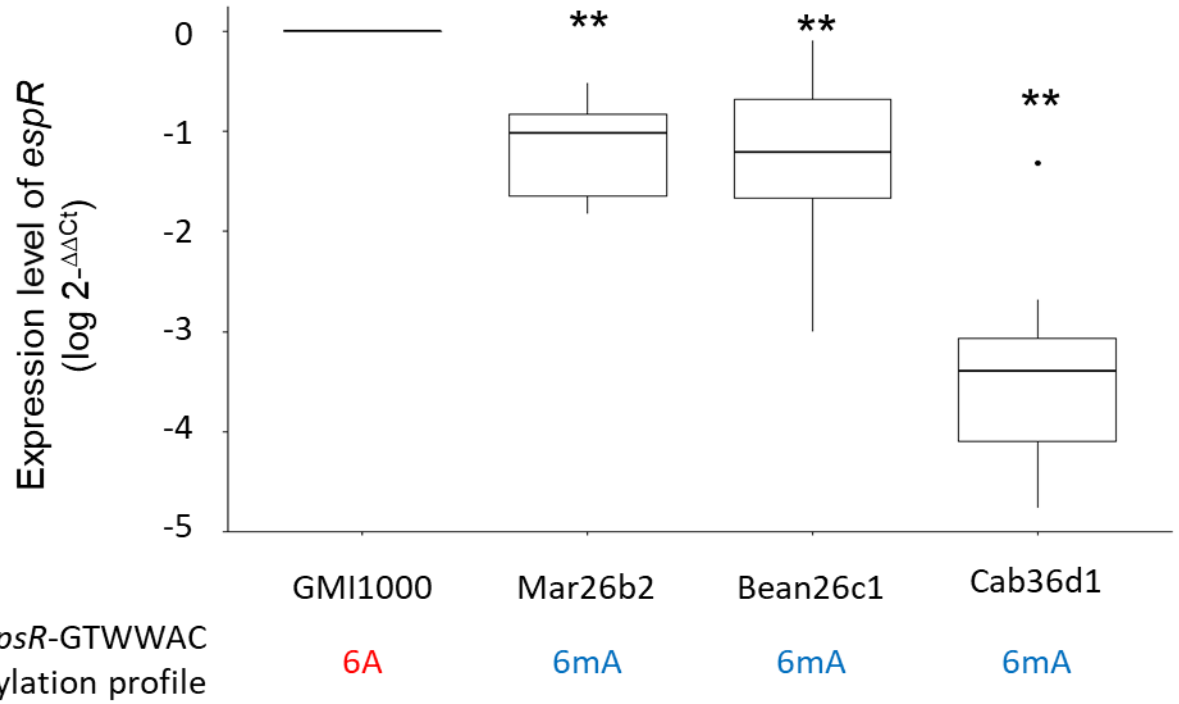
Expression level of espR
(log 2-ΔΔCt)
0
-1
-2
-3
-4
-5
**
**
**
GMI1000
Mar26b2
Bean26c1
Cab36d1
epsR-GTWWAC
Methylation profile
6A
6mA
6mA
6mA

Figure 3

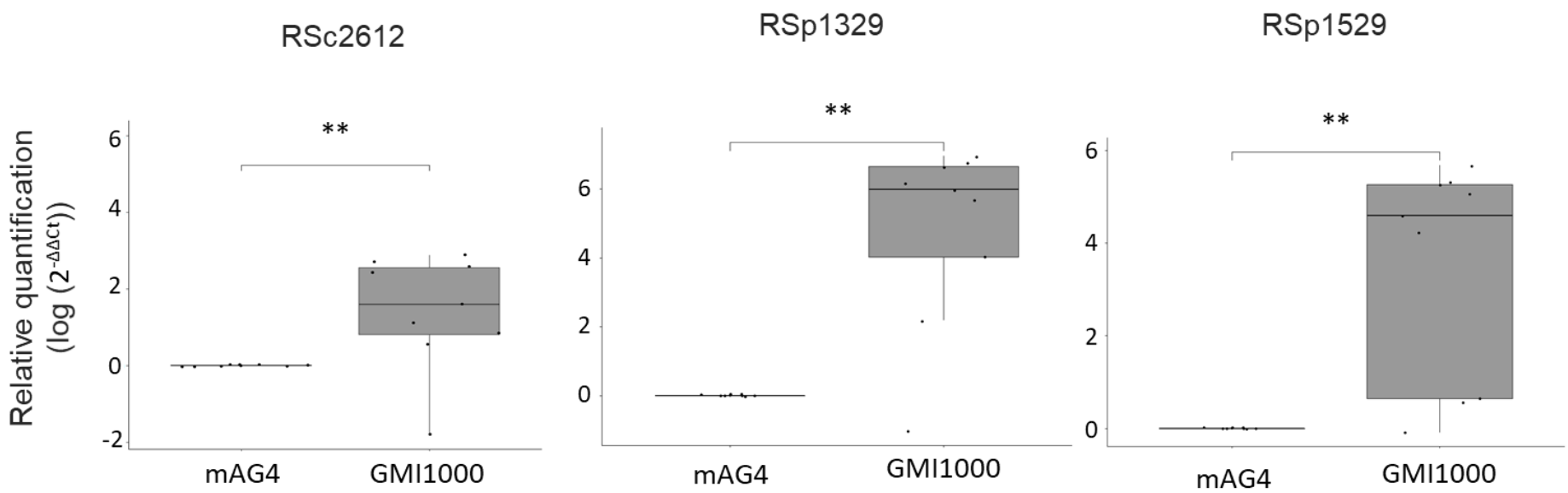
RSc2612
RSp1329
RSp1529
Relative quantification
(log (2-ΔΔCt))
**
6
4
2
0
-2
mAG4
GMI1000

Figure 4

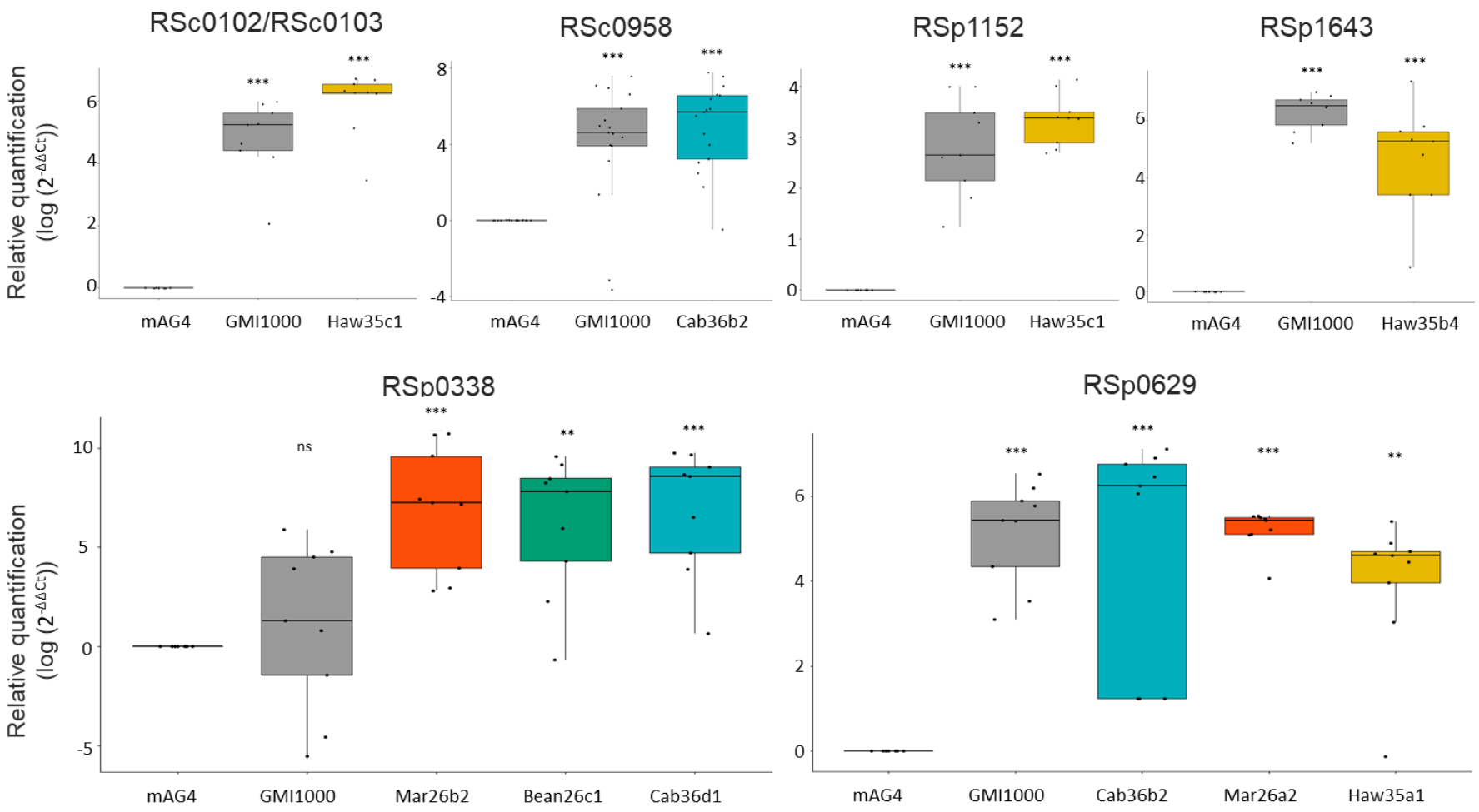
RSc0102/RSc0103
RSc0958
RSp1152
RSp1643
Relative quantification (log (2-ΔΔCt))
mAG4
GMI1000
Haw35c1
Cab36b2
Haw35b4
RSp0338
RSp0629
ns
Mar26b2
Bean26c1
Cab36d1
Mar26a2
Haw35a1

Figure 5

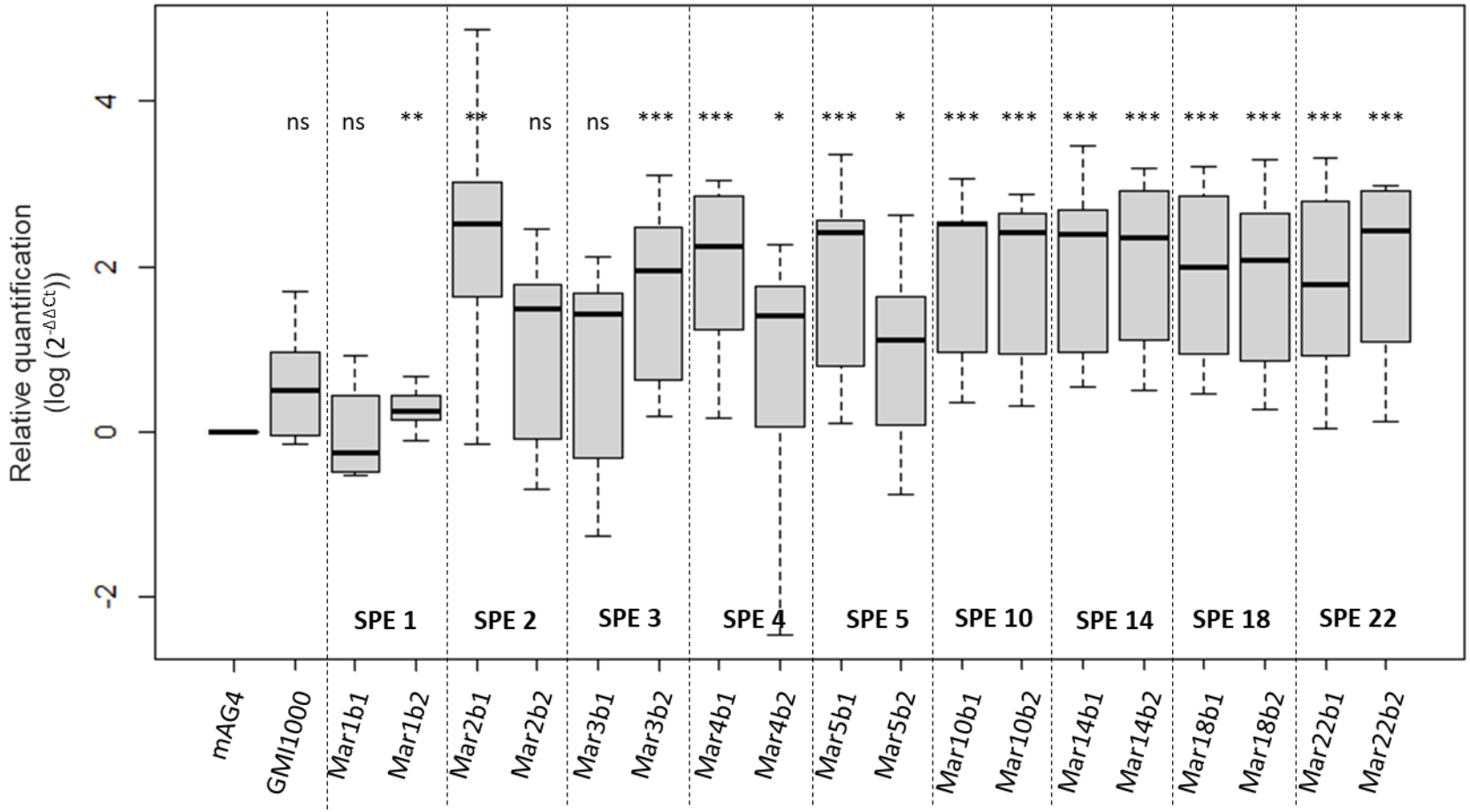
Relative quantification
(log (2^-ΔΔCt))
-2
0
2
4
ns
ns
**
**
ns
ns
***
***
*
***
*
***
***
***
***
***
***
***
***
***
SPE 1
SPE 2
SPE 3
SPE 4
SPE 5
SPE 10
SPE 14
SPE 18
SPE 22
mAG4
GMI1000
Mar1b1
Mar1b2
Mar2b1
Mar2b2
Mar3b1
Mar3b2
Mar4b1
Mar4b2
Mar5b1
Mar5b2
Mar10b1
Mar10b2
Mar14b1
Mar14b2
Mar18b1
Mar18b2
Mar22b1
Mar22b2

792 **Figure 6**

793

794

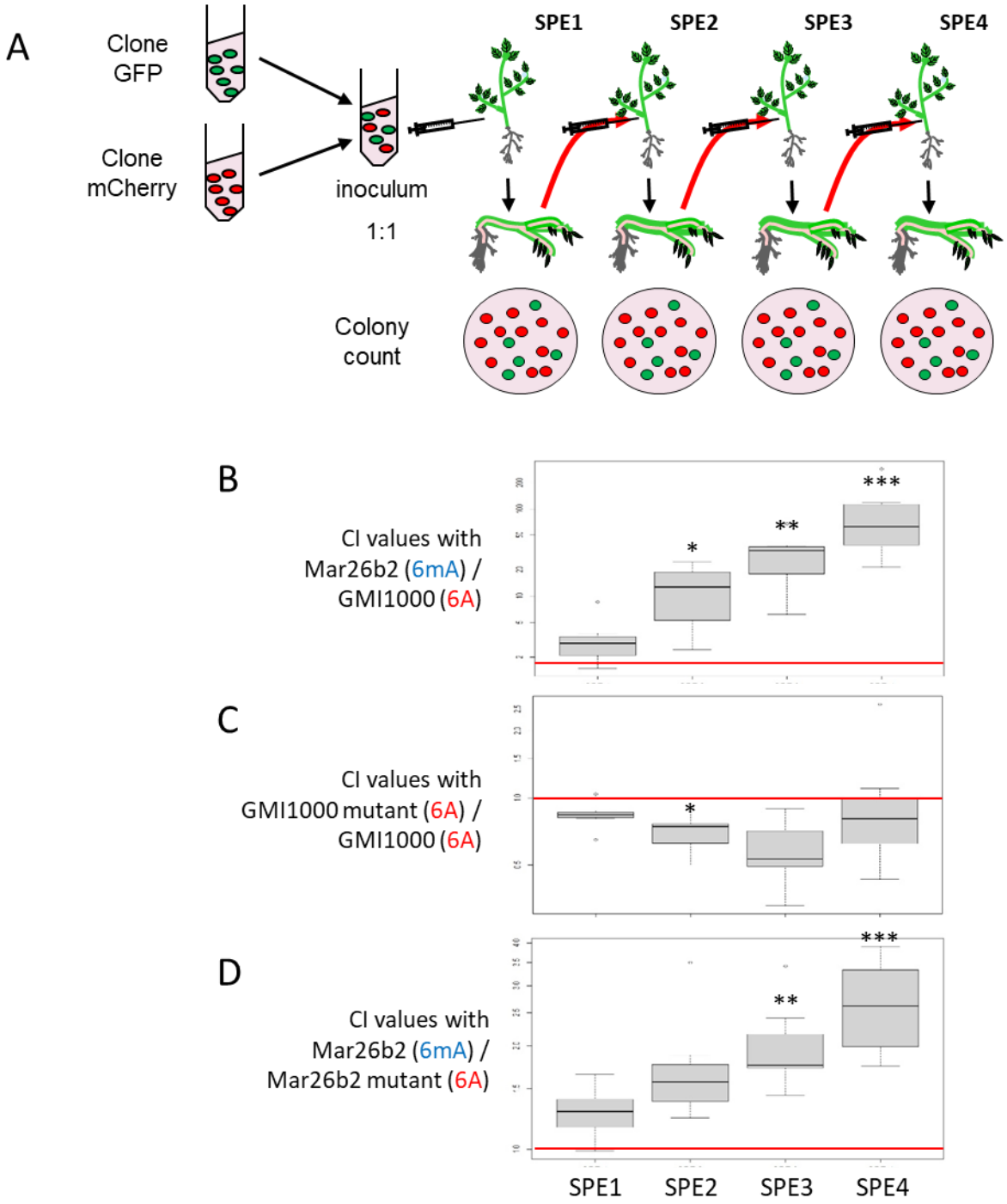

795

796